OPTIMAL DESIGN PROBLEMS IN THIN-FILM AND DIFFRACTIVE OPTICS

By

Yuliang Wang

A DISSERTATION

Submitted to
Michigan State University
in partial fulfillment of the requirements
for the degree of

Applied Mathematics - Doctor of Philosophy

2013

ABSTRACT

OPTIMAL DESIGN PROBLEMS IN THIN-FILM AND DIFFRACTIVE OPTICS

By

Yuliang Wang

Optical components built from thin-film layered structures are technologically very important. Applications include but are not limited to energy conversion and conservation, data transmission and conversion, space technology, imaging and so on. In practice these structures are defined by various parameters such as the refractive-index profile, the layer thickness and the period. The problem to find the combination of parameters which yield the spectral response closest to a given target function is referred to as optimal design. This dissertation considers several topics in the mathematical modeling and optimal design of these structures through numerical optimization.

A key step in numerical optimization is to define an objective function the measures the discrepancy between the target performance and that of the current solution. Our first topic is the impact of the objective function, its metric in particular, on the optimal solution and its performance. This is done by numerical experiments with different types of antireflection coatings using two-material multilayers. The results confirm existing statements and provide a few new findings, e.g. some specific metrics can yield particularly better solutions than others.

Rugates are optical coatings presenting continuous refractive-index profiles. They have received much attention recently due to technological advances and their potential better optical performance and environmental properties. The Fourier transform method is a widely used technique for the design of rugates. However, it is based on approximate expressions

with strict assumptions and has many practical limitations. Our second topic is the optimal design of rugates through numerical optimization of objective functions with penalty terms. We found solutions with similar performance and novel solutions by using different metrics in the penalty term.

Existing methods used only local basis functions such as piece-wise constant or linear functions for the discretization of the refractive-index profile. Our third topic is the use global basis functions such as sinusoidal functions in the discretization. A simple transformation is used to overcome the difficulty of bound constraints and the result is very promising. Both multilayer and rugate coatings can be obtained using this method.

Diffraction gratings are thin-film structures whose optical properties vary periodically along one or two directions. Our final topic is the optimal design of such structures in the broadband case. The objective functions and their gradient are obtained by solving variational problems and their adjoints with finite element method. Interesting phenomena are observed in the numerical experiments. Limitations and future work in this direction are pointed out.

ACKNOWLEDGMENTS

I would like to express my deep gratitude and appreciation to my dissertation advisor, Prof. Gang Bao for his support, understanding, encouragement, and patient guidance over the long term of my graduate study.

I would also like to thank my committee members Prof. Jianliang Qian, Prof. Chang Yi Wang and Prof. Zhengfang Zhou for their valuable kindness and help.

It is a great pleasure to thank my colleagues and friends for their solicitude and helpful suggestions.

TABLE OF CONTENTS

LIST OF FIGURES

Chapter 1

Introduction

For almost any practical applications of optics we will encounter a situation when light travels from one medium to another. In the optical community, one calls the input light the incident light. The medium from which the incident light propagates is called the incident medium and the other medium is called the substrate. The behavior of an incident light is completely determined once the properties of the incident medium and the substrate are given. An optical coating is defined as an additional layer of medium inserted between the two media in order to alter the behavior of incident light and achieve certain optical effects, such as reduction or enhancement of reflections. This work is concerned with the optimal design of optical coatings by numerical methods. The coatings considered are divided into two major types: classical thin-film coatings and diffraction gratings.

A thin-film coating consists of stratified media so that its optical properties vary in the direction normal to the interface but are invariant in the plane parallel to the interface. Probably the easiest way to obtain a thin-film optical coating is by putting a drop of oil on the surface of water. The interference effects at the interfaces between air, the oil film and water causes variation of reflectance with respect to wavelength and forms the colors as we see. The non-uniformity of the color is due to the non-uniformity of the thickness of the film and the fact that interference effects changes with the thickness. A similar example is soap bubble, in which case the coating medium is soap water and air plays the role of both

incident medium and substrate.

The coatings just mentioned have no practical application except producing beautiful color patterns. For a coating to be useful, one need have control over its parameters. The simplest possible coating would be consisting a single homogeneous layer. From the basic optical theory for stratified media, such a coating will reduce the reflectance to zero if its refractive index is $\sqrt{n_a n_s}$ and its optical thickness is one fourth of the wavelength. Here n_a, n_s denotes the refractive indices of the incident medium and substrate respectively.

The optical effects which can be achieved by a single homogeneous layer is very simple and limited. Mathematically speaking, this is because such a coating has only two parameters that can be tuned: its refractive index and thickness[1]. To achieve more complex effects, one need to increase the number of parameters of the coating. The most intuitive way to accomplish this is to use a stack of homogeneous layers. The coatings obtained this way are called multilayer coatings, often abbreviated "multilayers".

Multilayers have been successfully designed and produced to fulfill a wide range of purposes. Today multilayer coatings are employed in most antireflection coatings, dielectric mirrors, bandpass filters and various other optical devices. These devices have wide applications in many scientific and industrial areas such as astronomy, biology, medicine, energy conversion and conservation, data conversion and transmission, space technology, imaging, photography and so on.

The determination of the optical properties of a given multilayer is regarded as a forward problem. The optical properties just mentioned can refer to the relationship of the amplitude,

---

[1]The number of parameters will be three if permittivity and permeability can be tuned independently. This may be achievable with modern technology, but it is out of the scope of this work. Moreover we assume the real and imaginary parts of the refractive index can not be changed independently.

phase, angle, energy and polarization states of the reflected, transmitted and absorbed light on those of the incident light. The forward problem is well-posed in the sense that the solution is existent, unique and stable with respect to the input parameters. The theory and techniques for solving the this forward problem is relatively complete. However, the accuracy and efficiency of the solution methods are still very important issues since the optimal design problems usually requires solving a large number forward problems. In chapter we shall summarize the basic theory and techniques pertaining to the optimal design problems.

Conversely, the determination of multilayers that yield desired optical properties is regarded as an inverse problem. Unlike forward problems, inverse problems are usually ill-posed, namely the solutions may not be existent, unique or stable with respect to the input parameters. In particular, inverse problems for practical optical coatings usually have no exact solution. Consequently we have the take the second best and look for approximate solutions whose output are as close as possible to the desired ones. This is termed as optimal design problems.

Optimal design problems can be considered as generalized inverse problems and share some common properties with the latter, such as the non-uniqueness of solutions and their high sensitivity with respect to the target performance. In general these properties are considered as disadvantages for an inverse problem since its objective is to determine the solution, and the solution should be as accurate as possible. However, they could be advantages for an optimal design problem since its objective is to find solutions yielding the best performance. Non-uniqueness means we can have different designs giving the same performance, which is beneficial since we have an opportunity to select the best feasible one. High sensitivity of the solution with respect to the performance implies low sensitivity of the performance with respect to the solution, an advantage in practice indeed.

3

Before computers became powerful and cheaply available, multilayers are designed by analytic techniques such as the vector method, the Herpin index, the method of effective interfaces, the Smith's chart and so on. A complete account of these and other similar methods can be found in the books by Furman and Tikhonravov [1], Macleod [2] and the references cited therein. The analytic methods are intrinsically limited to small number of layers and simple target specifications. In addition, they can not be considered as optimal design methods. However, they are still useful today since they can provide insight and intuitive explanations which are generally lacking in numerical methods. In particular, the solutions obtained by analytic methods can be used as initial guess for numerical optimization methods.

The advances of modern computers boosts the development of numerical methods, numerical optimization methods in particular. Baumeister [3] is probably the first one to employ numerical optimization methods in the design of optical coatings. Since then many standard algorithms have been investigated for their applications in the optimal design of multilayers. For example, Dobrowolsk [4] applied and compared ten algorithms, including both deterministic and stochastic types. There exist various algorithms developed specifically for multilayers, too. One of the most notable is the so called needle method, originally proposed by Tikhonravov [5] and then developed and matured by himself and others. This method has been shown effective in the design of multilayers for a wide range of applications. However, none of the methods can claim to be the best for all cases due to the variety of the applications. In this work we shall not consider the problem of finding or devising the best algorithm for all design problems.

A key step in solving a practical problem by numerical optimization is to define an objective function to be minimized. The objective function should measure the discrepancy

4

between the target performance and that of the current solution. The metric in which the discrepancy is measured will certainly affect the solutions and their performance. Chapter is devoted to our study on this subject. We will demonstrate the impact of the metrics through numerical examples and observe both anticipated and unanticipated phenomena. Practical implication and value of the observations will be pointed out.

As mentioned earlier, using a stack of homogeneous layers is one way to increase the degree of freedom of a thin-film structure so as to achieve complex and powerful optical effects. Another approach to accomplish the goal is to use a single inhomogeneous, mostly continuous layer. The coatings obtained this ways are called rugate coatings, often abbreviated "rugates". Traditionally rugates refer to coatings whose refractive-index profiles are constructed from sinusoidal and other elementary functions and which are much thicker than their multilayer counterparts. Oftentimes this name is used interchangeably with "gradient-index coatings" and "inhomogeneous coatings", both of which refer to coatings with arbitrary continuous refractive-index profiles and similar thickness compared to multilayers. We shall pose no restrictions on the thickness of coatings and use "rugates" for all coatings with continuous refractive-index profiles.

Rugates have received much attention recently due to their better environmental properties, less sensitivity to production errors and potential better optical performances in complicated situations. The Fourier transform method is a widely used and powerful technique for the design of rugates. However, it is based on approximate expressions with strict assumptions and is restricted to single incident angle and polarization state. Another approach is to divide the coating into a large number of thin homogeneous layers and optimize an objective function with respect to the refractive indices of all layers. Because of the maximum principle of thin-film optics [6], the coatings obtained this ways generally resemble multilayers

5

or possess many discontinuous points if the usual objective functions are applied. In order to force smoothness to the solutions, we add penalty terms to the usual objective functions. In chapter we study these methods and obtain similar solutions as other methods and new ones never seen before by using different norms in the penalty terms.

Existing optimization methods for the optimal design of thin-film coatings have used only local basis functions (step and hat functions) for the parameterization of the refractive-index profile. Global basis functions such as sinusoidal functions have been used only in heuristic design methods. In chapter we propose a method to use a global basis functions in the design of optical coatings. The problem of using global basis functions in this context is that there is no direct way to translate the bound constraints on the refractive-index profile to its spectral coefficients. We overcome this difficulty by a simple transformation of the bounded functions to unbounded ones. This way the truncated series expansion can be used to approximate the coating profile and unconstrained optimization algorithms can be used on the series coefficients. An interesting feature of this method is that we can obtain both rugates and multilayers with very similar performances.

So far we considered only optical coatings built from layer structures. The refractive index of such structures vary along one direction and is homogeneous over the other two. By allowing the refractive index of the structure to vary periodically along one or both of the other two directions one obtains singly or doubly periodic structures, often called 2D or 3D diffraction gratings, respectively. Dobson studied the optimal design of wide-angle antireflective diffraction gratings [7] and blazed diffraction gratings [8]. Following the spirit of these work, we study the optimal design of broadband antireflective diffraction gratings in chapter . The value and gradient of the objective function was obtained by solving a 2D PDE with nonlocal transparent boundary conditions [9] and the corresponding adjoint

equation [7], respectively.

Chapter 2

Basic Theory for Thin-film Optics

The basic theory for thin-film optics can be found from a few texts, such as Born and Wolf [10], Furman [1] and Macleod [2]. In this chapter we summarize the parts of the theory that are essential and necessary for our work. We start from the Maxwell's equations and derive the formulas to compute the reflectance, transmittance and their derivatives with respect to the layer thicknesses and refractive indices of a multilayer system.

2.1 Maxwell's Equations

The behavior of light, and electromagnetic field in general, is described by the Maxwell's equations (in the Gaussian system of units):

$$\nabla \times \mathcal{H} - \frac{1}{c}\frac{\partial \mathcal{D}}{\partial t} = \frac{4\pi}{c}\mathbf{j}, \tag{2.1a}$$

$$\nabla \times \mathcal{E} + \frac{1}{c}\frac{\partial \mathcal{B}}{\partial t} = 0, \tag{2.1b}$$

$$\nabla \cdot \mathcal{D} = 4\pi\rho, \tag{2.1c}$$

$$\nabla \cdot \mathcal{B} = 0, \tag{2.1d}$$

where

$\mathcal{E}$	electric vector
$\mathcal{H}$	magnetic vector
$\mathcal{D}$	electric displacement
$\mathcal{B}$	magnetic induction
$\mathbf{j}$	electric current density
ρ	electric charge density
c	speed of light in vacuum

In the field of thin-film coatings the source terms $\mathbf{j}$ and ρ are assumed to be zero. In addition, the other four quantities $\mathcal{E}, \mathcal{H}, \mathcal{D}, \mathcal{B}$ must be supplemented by material equations for a unique determination of the field vectors. They are rather complicated in general. In this work we assume the body is moving at slow speed, the material is isotropic and linear, and the field is time harmonic. Under these assumptions the material equations are give by

$$\mathcal{D} = \varepsilon \mathcal{E},$$

$$\mathcal{B} = \mu \mathcal{H}.$$

where ε and μ are called the relative permittivity and permeability respectively.

We assume the field is time harmonic and write

$$\mathcal{E} = \mathbf{E} \exp(-i\omega t),$$

$$\mathcal{H} = \mathbf{H} \exp(-i\omega t),$$

where ω is the angular frequency of the field.

Applying all the above assumptions to (2.1) we arrived at these equations

$$\nabla \times \mathbf{E} - ik\mu\mathbf{H} = 0, \tag{2.2a}$$

$$\nabla \times \mathbf{H} + ik\varepsilon\mathbf{E} = 0, \tag{2.2b}$$

where $k = \omega/c$ is the wavenumber in vacuum. Notice $k = 2\pi/\lambda$ if λ is the wavelength in vacuum.

Finally we have the following boundary conditions at a surface of discontinuity:

$$\mathbf{n_{12}} \times (\mathbf{E_2} - \mathbf{E_1}) = 0, \tag{2.3a}$$

$$\mathbf{n_{12}} \times (\mathbf{H_2} - \mathbf{H_1}) = 0, \tag{2.3b}$$

where $\mathbf{n_{12}}$ is the normal vector of the surface from region 1 to region 2 and $\mathbf{E_j}, \mathbf{H_j}$ are the field vectors in region j respectively.

2.2   Model Equations for Layered Medium

For the sake of simplicity we also assume the material is nonmagnetic, namely the permeability $\mu = 1$ everywhere, so that the problem geometry is characterized completely by the permittivity ε. A thin-film coating consists a layered medium of finite depth sandwiched

between two homogeneous media of infinite depth. In other words, we have

$$\varepsilon(x, y, z) = \begin{cases} \epsilon_a, & z \leq 0, \\ \epsilon(z), & 0 < z < L, \\ \epsilon_s, & z \geq L. \end{cases}$$

The medium occupying the region $z \leq 0$ is called the incident medium and the medium occupying the region $z \geq L$ is called the substrate. The incident medium is where the source light (incident light) comes from. We assume the incident light is a plane wave, namely the field vectors $\mathbf{E}, \mathbf{H}$ have spatial dependence $\exp(i\mathbf{k} \cdot \mathbf{r})$ where $\mathbf{k}$ is a wave vector with $|\mathbf{k}| = k\sqrt{\varepsilon_a}$ and $\mathbf{r} = (x, y, z)$ is the spatial vector. Notice $\mathbf{k}$ is the direction of propagation of the light. Due to the invariance of ε along the x, y axes, any plane wave solution of (2.2) can be decomposed into two components called transverse-electric (TE) and transverse magnetic (TM) modes, respectively.

The plane formed by the propagation direction $\mathbf{k}$ and the z-axis is termed the incident plane. Since ε is invariant along both x and y axes, we assume the incident plane is the yz plane without loss of generality. In the case of TE mode, the electric field is perpendicular to the incident plane. So $\mathbf{E}$ has only the x-component different from zero. Let us write $\mathbf{E} = (u, 0, 0)$ and substitute it into (2.2). Expanding the $\nabla \times$ operators we find $\mathbf{H}$ lies in the yz plane and is independent on x. Hence u is also independent on x and we can write $u = u(y, z)$. The resultant equation for u is the following:

$$(\Delta + k^2 \varepsilon)u = 0, \tag{2.4}$$

where $\Delta = (\partial_{yy} + \partial_{zz})$. By the variable separation method we find

$$u(y, z) = u(z) \exp(ik\alpha y),$$

where α is a constant to be determined. Substituting this to (2.2) yields

$$\mathbf{H} = (0, -v(z), \alpha u(z)) \exp(ik\alpha y),$$

where v and u are solutions to the following system of linear ordinary differential equations:

$$\frac{du}{dz} = ikv, \tag{2.5a}$$

$$\frac{dv}{dz} = ik(\varepsilon - \alpha^2)u. \tag{2.5b}$$

To determine the value of α, consider the wave in the incident medium. If the incident angle is θ_I, then the wavevector

$$\mathbf{k} = k\sqrt{\varepsilon_a}(0, \sin\theta_I, -\cos\theta_I)$$

and

$$u(y, z) = \exp(ik\sqrt{\varepsilon_a})(y \sin\theta_I - z \cos\theta_I).$$

Hence $\alpha = \sqrt{\varepsilon_a} \sin\theta_I$.

In the case the TM mode, the $\mathbf{H}$ field is perpendicular to the incident plane and we can write $\mathbf{H} = (u(z), 0, 0)$. Similar to the case of TE mode, we find

$$\mathbf{E} = \left(0, v(z), -\frac{\alpha}{\varepsilon}u(z)\right) \exp(ik\alpha y),$$

and u, v are solutions to the following system of linear ordinary differential equations

$$\frac{du}{dz} = ik\varepsilon v, \tag{2.6a}$$

$$\frac{dv}{dz} = ik\left(1 - \frac{\alpha^2}{\varepsilon}\right)u. \tag{2.6b}$$

2.3 Reflectance and Transmittance

Now we derive formulas for the reflectance and transmittance for a layered structure. Let us assume TE mode for the time being. For the sake of convenience let us normalize the field so that the electric field at the substrate interface $u(L) = 1$. Denote u_I, v_I, u_R, v_R to be the field of the incident wave and reflected wave respectively. By (2.5) we obtain

$$v_I(0) = q_a u_I(0),$$
$$\tag{2.7}$$
$$v_R(0) = -q_a u_R(0),$$

where $q_a = \sqrt{\varepsilon_a - \alpha^2}$. By the jump conditions (2.3) we obtain the continuity of u, v at the interface $z = 0$. As a result, we have

$$u(0) = u_I(0) + u_R(0),$$

$$v(0) = v_I(0) + v_R(0) = q_a(u_I(0) - u_R(0)).$$

Solving the above system for $u_I(0)$ and $u_R(0)$ we obtain the following

$$u_I(0) = \frac{q_a u(0) + v(0)}{2q_a},$$

$$u_R(0) = \frac{q_a u(0) - v(0)}{2q_a},$$

13

The amplitude reflectance r is defined to be the ratio of the tangential component of the electric field of the reflected wave and incident wave. Hence we obtain r in terms of the total field at the incident interface $z = 0$:

$$r = \frac{u_R(0)}{u_I(0)} = \frac{q_a u(0) - v(0)}{q_a u(0) + v(0)}. \tag{2.8}$$

Similarly we obtain the amplitude transmittance t in terms of the total field at the substrate interface $z = L$:

$$t = \frac{u(L)}{u_I(0)} = \frac{2q_a}{q_a u(0) + v(0)}. \tag{2.9}$$

Now consider the special case when the coating layer is homogeneous, namely we assume $\varepsilon(z) = \varepsilon, 0 < z < L$. For the sake of convenience we introduce the refractive index $n = \sqrt{\varepsilon}$. Eliminating v from (2.5) yield the Helmholtz equation for u:

$$\frac{d^2 u}{dz^2} + k^2(n^2 - \alpha^2)u = 0. \tag{2.10}$$

Denote $\beta^2 = k^2(n^2 - \alpha^2)$, then the general solution of the above equation is the following

$$u(z) = c_1 \exp(i\beta z) + c_2 \exp(-i\beta z).$$

From the first equation in (2.5) we obtain

$$v(z) = q(c_1 \exp(i\beta z) - c_2 \exp(-i\beta z)),$$

where we denote $q = \dfrac{\beta}{k}$. Substituting $z = 0$ and $z = L$ in the above solutions respectively and eliminating c_1, c_2, we obtain the following equation relating the field values at the substrate

14
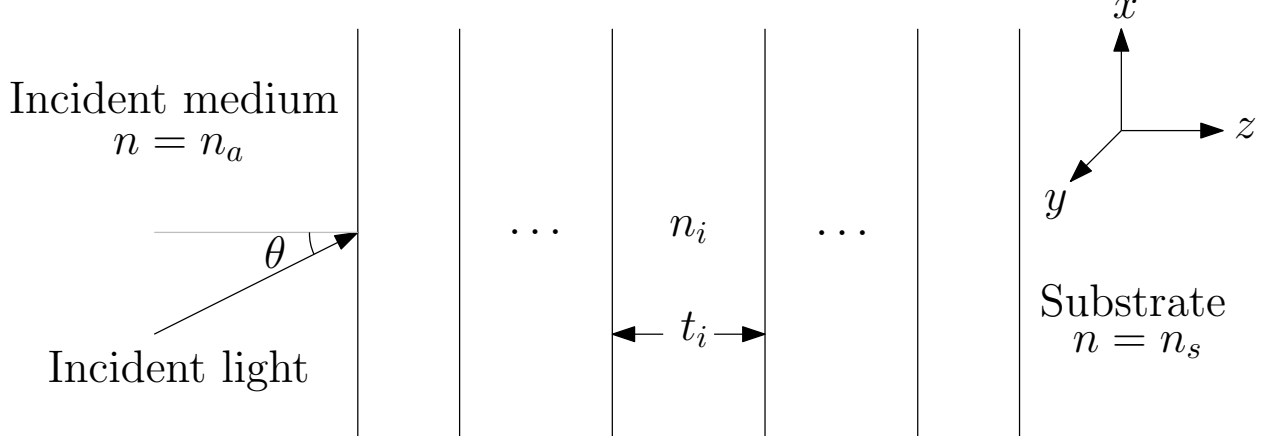
Figure 2.1: Problem geometry for multilayer coatings.

interface to those at the incident interface:

$$
\begin{bmatrix} u(0) \\ v(0) \end{bmatrix} = \begin{bmatrix} \cos(\beta L) & -\dfrac{i}{q}\sin(\beta L) \\ -iq\sin(\beta L) & \cos(\beta L) \end{bmatrix} \begin{bmatrix} u(L) \\ v(L) \end{bmatrix}
\tag{2.11}
$$

Let $u(L) = 1$, then $v(L) = q_s = \sqrt{\varepsilon_s - \alpha^2}$ from continuity. Plugging these into (2.11) we obtain $u(0), v(0)$. Together with (2.8) and (2.9) we can write the expressions for the amplitude reflectance r and amplitude transmittance t.

Now consider a multilayer coating with layer thicknesses $\{t_1, \cdots, t_n\}$ and refractive indices $\{n_1, \cdots, n_N\}$ (See Figure 2.1). Combining (2.11) for all layers we obtain

$$
\begin{bmatrix} u(0) \\ v(0) \end{bmatrix} = \left(\prod_{j=1}^{N} M_j \right) \begin{bmatrix} u(L) \\ v(L) \end{bmatrix}, \quad M_j = \begin{bmatrix} \cos(\beta_j t_j) & -\dfrac{i}{q_j}\sin(\beta_j t_j) \\ -iq_j\sin(\beta_j t_j) & \cos(\beta_j t_j) \end{bmatrix}, \tag{2.12}
$$

where $L = \sum_{j=1}^{n} t_j$, $\beta_j = \sqrt{n_j^2 - \alpha^2}$ and $q_j = \dfrac{\beta_j}{k}$. Then we can calculate r and t as in the single layer case. This technique for the computation of reflectance and transmittance of a multilayer is called the matrix method and will be used through out this work for the

15

computation of the objective functions.

In order to use gradient based optimization algorithms such as quasi-newton methods, one need the gradient of the objective functions, which in turn are computed from the gradient of r and t. From (2.8) and (2.9) we see the gradient of r and t can be expressed in terms of the gradient of $u(0)$ and $v(0)$, which can be easily obtained from (2.12) since each parameter t_{j_0} and n_{j_0} appears only in M_{j_0}. Therefore we have

$$\frac{d}{dt_{j_0}} \begin{bmatrix} u(0) \\ v(0) \end{bmatrix} = \left(\prod_{j=1}^{j_0-1} M_j \right) \frac{dM_{j_0}}{dt_j} \left(\prod_{j=j_0+1}^{N} M_j \right) \begin{bmatrix} u(L) \\ v(L) \end{bmatrix}, \qquad \text{(2.13a)}$$

$$\frac{d}{dn_{j_0}} \begin{bmatrix} u(0) \\ v(0) \end{bmatrix} = \left(\prod_{j=1}^{j_0-1} M_j \right) \frac{dM_{j_0}}{dn_j} \left(\prod_{j=j_0+1}^{N} M_j \right) \begin{bmatrix} u(L) \\ v(L) \end{bmatrix}. \qquad \text{(2.13b)}$$

The computational cost for r and t is $\mathcal{O}(N)$ due to multiplication of N 2×2 matrices. The computational cost for each partial derivatives is also $\mathcal{O}(N)$ and the computational cost for the gradient will be $\mathcal{O}(N^2)$ if done straightforwardly using (2.13). The cost can be reduced to $\mathcal{O}(N)$ once we notice the matrix products

$$\prod_{j=1}^{j_0-1} M_i, \ \prod_{j=j_0+1}^{N} M_j.$$

can be computed progressively, once in forward direction and another in the backward direction, as noted by, e.g. Verly [11]. In addition, we utilized the Armadillo C++ linear algebra library [12] for computation of matrix multiplications due to its exceptional efficiency in handling small matrices.

Finally, in many practical situations we are concerned with only the energy carried in the reflected and transmitted waves. The magnitude and direction of the energy carried by

a time-harmonic EM wave is given by the time-averaged Poynting vector

$$\mathbf{S} = \frac{c}{8\pi}\Re(\mathbf{E}\overline{\mathbf{H}}).$$

Using out notations the energy carried by the wave along the z-axis is given by

$$S_z = \frac{c}{8\pi}\Re(uv).$$

From (2.7) we find the energy carried by the incident and reflected wave along the z-axis is given by

$$\frac{c}{8\pi}\Re(q_a)|u_I(0)|^2, \quad -\frac{c}{8\pi}\Re(q_a)|u_R(0)|^2,$$

respectively. The power reflectance R is defined by the ratio of the energy carried by the reflected wave along the z-axis to that of the incident wave. Thus we have

$$R = |r|^2. \tag{2.14}$$

Similarly we can derive the formula for the power transmittance:

$$T = \frac{\Re(q_s)}{\Re(q_a)}|t|^2. \tag{2.15}$$

The gradient of R and T with respect to layer thicknesses and refractive indices are computed

easily from those of r and t:

$$\nabla R = 2\Re(r\nabla r), \tag{2.16a}$$

$$\nabla T = 2\frac{\Re(q_s)}{\Re(q_a)}\Re(t\nabla t). \tag{2.16b}$$

Chapter 3

Norm of Objective Functions

In this chapter we consider the optimal design of two-material multilayer AR coatings. The most common approach to this problem is numerical optimization. Baumeister [3] seems to be the first one to employ this approach. Since then people have investigated various existing optimization algorithms and developed many new ones. For example, ten different algorithms of deterministic and stochastic types were tested and compared in [4]. The needle method proposed in [5] is one of the most powerful algorithms. It has been successfully used in the design of not only antireflection but also other complicated optical coatings.

Besides the conventional stratified thin-film coatings, numerical methods have been studied and successfully applied to the optimal design of other thin-film structures, such as diffraction gratings with specified diffraction patterns [13, 14, 15, 9, 8] and with omnidirectional antireflection properties [7], guided-mode grating resonant structures [16, 17, 18] and nonlinear diffraction gratings [19].

A key step in numerical optimization is to define a merit function that measures the discrepancy between the target and and solution. The metric in which the discrepancy is measured will certainly affect the optimal solution and its performance. The most commonly used metric is of the least-square type. Others include the sum of residuals or the max of the residuals. For broadband AR coatings, the merit functions corresponding to the previously

mentioned metrics are given by

$$\left\{ \frac{1}{M} \sum_{i=1}^{M} [R(k_i)]^2 \right\}^{\frac{1}{2}}, \quad \frac{1}{M} \sum_{i=1}^{M} R(k_i), \quad \max_{1 \le i \le M} R(k_i),$$

where $R(k_i)$ denotes the reflectance at wavenumber k_i and $\{k_i : 1 \le i \le M\}$ is a set of uniformly distributed sampling points in the spectral region of interest.

Mathematically speaking, these can be considered as discrete approximations of the L^2, L^1 and L^∞ norms of the function $R(k)$ over the spectral region. Naturally we can also consider using L^p norms for other positive integers p. It was mentioned in [20] that greater p will force solutions which tend to equalize the residuals. However, no theoretical or numerical substantiations have been made.

In this chapter we conduct quantitative studies on the impact of p on the optimal design of antireflection coatings . This is accomplished by comparing the average and maximal values of the reflected power over the spectral and/or angular regions of interest through numerical experiments. These specific values are chosen because they are the most important for many practical applications. The average value, up to a weight function, measures the average power reflected by the interface. Thus it is more important than other quantities in situations when maximal power absorption is mostly desired, e.g. solar cell panels. On the other hand, imaging devices such as glasses and camera lenses should be designed so that the reflected power is more evenly spread and the maximal value is as small as possible.

3.1 Formulation and Algorithms

Without loss of generality, the AR coating will be assumed to be of broadband type in this section. Formulations for omnidirectional and broadband-and-omnidirectional types are similar. The spectral region of interest will be denoted by an interval $[k_L, k_H]$ of wavenumber or an interval $[\lambda_L, \lambda_H]$ of wavelength. Wavenumber is better suited in mathematical formulation while wavelength seems to be more natural in the description of practical applications. Let $\{k_i : 1 \leq i \leq M\}$ be a set of uniformly distributed points in $[k_L, k_H]$ with $k_0 = k_L$ and $k_M = k_H$ and define a class of merit functions $\{f_p : 1 \leq p \leq \infty\}$ by

$$
f_p = \begin{cases} \left\{ \dfrac{1}{N} \displaystyle\sum_{i=1}^{N} [R(k_i)]^p \right\}^{\frac{1}{p}}, & \text{if } p < \infty, \\[2em] \displaystyle\max_{1 \leq i \leq N} R(k_i), & \text{if } p = \infty, \end{cases} \tag{3.1}
$$

where R is reflectance as a function of wavenumber. Dispersion of all materials are ignored in the calculation of f_p and its gradient, although it can be incorporated into our model through simple transformations as in [21].

The value of f_p can be computed directly from the values of $R(k_i)$ for all p. The partial derivatives of f_p can be computed directly from the values of $R(k_i)$ and their partial derivatives for $p < \infty$. The function f_∞, on the other hand, is not differentiable. In order to use gradient-based optimization algorithms, we transform the original optimization problem

$$
\min_{\mathbf{L}} \max_{1 \leq i \leq N} R(\mathbf{L}, k_i)
$$

into an equivalent form:

$$\min_{\mathbf{L}} s \text{ subject to } R(\mathbf{L}, k_i) - s \leq 0 \ \forall i, \tag{3.2}$$

where $\mathbf{L} = \{t_1, \cdots, t_N\}$ is the design variable. The equivalence of these two problems is shown in e.g. [22] and it is the approach adopted in [23]. Note that the objective function and all the constraint functions in (3.2) are differentiable. Different approaches have been proposed in [24, 25]. They are more complicated but can be used to design other types of coatings.

Now that the optimization problems are completely setup, we need to choose algorithms. Although the needle method could be the best candidate, it is rather complicated compared with straightforward optimization algorithms. Since our objective is not to find the best algorithm but to study the impact of the metrics, we choose to utilize existing algorithms in the open source library NLopt [26]. All the local gradient-based algorithms in this library can handle cases for $p < \infty$. Among them we find the low-storage BFGS algorithm described in [27] to be particularly efficient for our test problems. If it fails to converge, we can always turn to more robust but less efficient ones. The only algorithm in this library that can handle nonlinear constraints is a sequential quadratic programming method based on the implementation in [28], so it is the one we shall use for the case $p = \infty$.

For two-material coatings, the refractive indices n_i take a low and high value alternatively. They are fixed up to the value of the first layer. Thus the design variables on which we do optimization are layer thicknesses t_i. For both practical and computational considerations, we need define lower and upper bounds for the design variables. First of all, we need set a lower bound, which must be non-negative in order to avoid nonphysical solutions. In fact, it

will be set to 0 in our numerical experiments. However, zero-thickness and thin layers could occur in the solution. Due to limited accuracy of equipment and sensitivity to manufacturing errors, thin layers should be avoided in the design. This can be achieved by specifying a positive value for the lower bound in the beginning or by a process named "consolidation" [29, 11], which eliminates thin layers during or after the optimization. There exist two possible approaches for this process: erase thin layers or merge them with neighboring thicker layers. Existing works did not mention which method is better and which one was used in their works. We tested both approaches and found the latter usually yields better results than the former. Our algorithm for the consolidation process is the following:

set thresholds T_i for $1 \leq i \leq N$;
for $i = 2$ **to** M **do**
    if $t_i < T_i$ **then**
        $n_i \leftarrow n_{i-1}$;
    end
    if $t_1 < T_1$ **then**
        $n_1 = n_2$;
    end
end
combine neighboring layers with the same refractive index

Algorithm 1: Consolidation of multilayer coatings.

The procedure "optimization $\rightarrow$ consolidation" is iterated until no thin layers remain. The thresholds t_i are user input values that specify the least thicknesses to be present in the coating and can be chosen independently for each layer. Obviously they should not be too large, since otherwise the obtained solution will be far from optimal. They can be very small so that only the layers with zero thicknesses are consolidated. Interestingly, by using suitable values we obtain coatings with much less layers but similar or even better performances.

An upper bound is not needed unless it is a required feature of the coating since our algorithms always generate solutions without too thick layers.

3.2 Numerical Experiments and Discussion

Besides the merit functions, the lowest achievable residual reflectance of an antireflection coating depends on many other parameters such as

- refractive indices of the coating material and the ambient media

- total number of layers

- total optical thickness

- spectral and/or angular regions

- state of polarization

An explicit formula for this dependence is not available, but some empirical expressions have been proposed in [30, 31, 32, 33]. For the purpose of our numerical experiments, these parameters will be held fixed when p is varied.

In all the following experiments, the refractive indices of the incident and substrate media are 1.0 and 1.52, corresponding to air and glass, while the low and high refractive indices of the two materials used in the coating are 1.45 and 2.35, respectively. The number of layers is set to 20 in the beginning and will be reduced in the final solutions due to the consolidation process.

Initial guesses play an important role for local optimization methods. We use a quarter-wave stack at a fixed wavelength λ_c. That is, we set $t_i = \lambda_c/(4n_i)$ for each i. In the case of broadband AR coatings, good results can be obtained if λ_c is slightly less than λ_L as suggested in [34]. According to our numerical experiments, smaller λ_c will cause more layers to have zero thicknesses during the optimization. This leads to less number of layers and

worse performance in the final solution. If λ_c is too small, all layers with refractive index n_H will be eliminated and the final solution consists of a single layer with refractive index n_L. On the other hand, the solution will be far from optimal if $\lambda_c > \lambda_L$. The best choice should be made by a trial-and-error method and is dependent on the specific problem. However, our numerical experience shows that the choice $\lambda_c = 0.8\lambda_L$ can produce good results consistently for many different combinations of parameters.

The above observations are true not only for the broadband type but also for the omnidirectional (with λ_0 playing the role of λ_L) and broadband-and-omnidirectional types. In all the results shown in the sequel we used the initial guesses with $\lambda_c = 0.8\lambda_L$.

As mentioned in section 3.1, the thickness thresholds t_i controls a balance between the performance and the minimal layer thickness of the final coating. We used $t_i = \lambda_L/(60n_i)$ for all the experiments.

We now present results for the following three AR coatings

(a) broadband: normal incidence over spectral region $[\lambda_L, \lambda_U] = [400, 1200]$

(b) omnidirectional: at fixed wavelength $\lambda_0 = 100$ over angular region $[\theta_L, \theta_H] = [0°, 90°]$

(c) broadband-and-omnidirectional: over the spectral region $[\lambda_L, \lambda_U] = [400, 1200]$ and angular region $[\theta_L, \theta_H] = [0°, 90°]$.

The merit functions for the three cases are defined as the following respectively:

$$
f_p = \begin{cases}
\left\{ \dfrac{1}{M} \displaystyle\sum_{i=1}^{M} [R(k_i)]^p \right\}^{\frac{1}{p}}, & \text{if } p < \infty, \\[2em]
\displaystyle\max_{1 \le i \le M} R(k_i) I(k_i), & \text{if } p = \infty,
\end{cases}
$$

$$
f_p = \begin{cases} \left\{ \dfrac{1}{N} \displaystyle\sum_{i=1}^{N} [R(\theta_i)\cos(\theta_i)]^p \right\}^{\frac{1}{p}}, & \text{if } p < \infty, \\[4ex] \displaystyle\max_{1 \le i \le N} R(\theta_i)\cos(\theta_i), & \text{if } p = \infty, \end{cases}
$$

$$
f_p = \begin{cases} \left\{ \dfrac{1}{MN} \displaystyle\sum_{i=1}^{M}\sum_{j=1}^{N} [R(k_i,\theta_j)\cos(\theta_j)]^p \right\}^{\frac{1}{p}}, & \text{if } p < \infty, \\[4ex] \displaystyle\max_{1 \le i \le M, 1 \le j \le N} R(k_i,\theta_j)\cos(\theta_j), & \text{if } p = \infty, \end{cases}
$$

where $\{k_1, \cdots, k_M\}$ and $\{\theta_1, \cdots, \theta_N\}$ are uniformly distributed sampling points in $[k_L, k_U]$ and $[\theta_L, \theta_U]$, respectively. Notice our definitions of merit functions for the omnidirectional and broadband-and-omnidirectional cases are different from conventional ones by a factor of $\cos(\theta_i)$. This factor is included so that the merit functions represent the reflection in the sense of total power. This difference is not essential for our discussion since it can be regarded as a weight function. The observations and conclusions in the sequel are still valid if this term is dropped out.

Notice that the average and maximal power of reflection P_{ave} and P_{max} are approximated by f_1 and f_∞ respectively. In fact, they are computed by the same formula except with with a larger number of sampling points in our experiments. Intuitively the values of P_{ave}, P_{max} should be the lowest when f_1, f_∞ are used as the merit functions and should increase and decrease as p increases when f_p are used as merit functions. These are generally the case as seen from Figure 3.1, where these values are plotted against p for $1 \le p \le 100$.

There are several other interesting phenomena associated with P_{ave} and P_{max} in Figure 3.1:

- The increase and decrease of the two values slows down quickly as p increases.
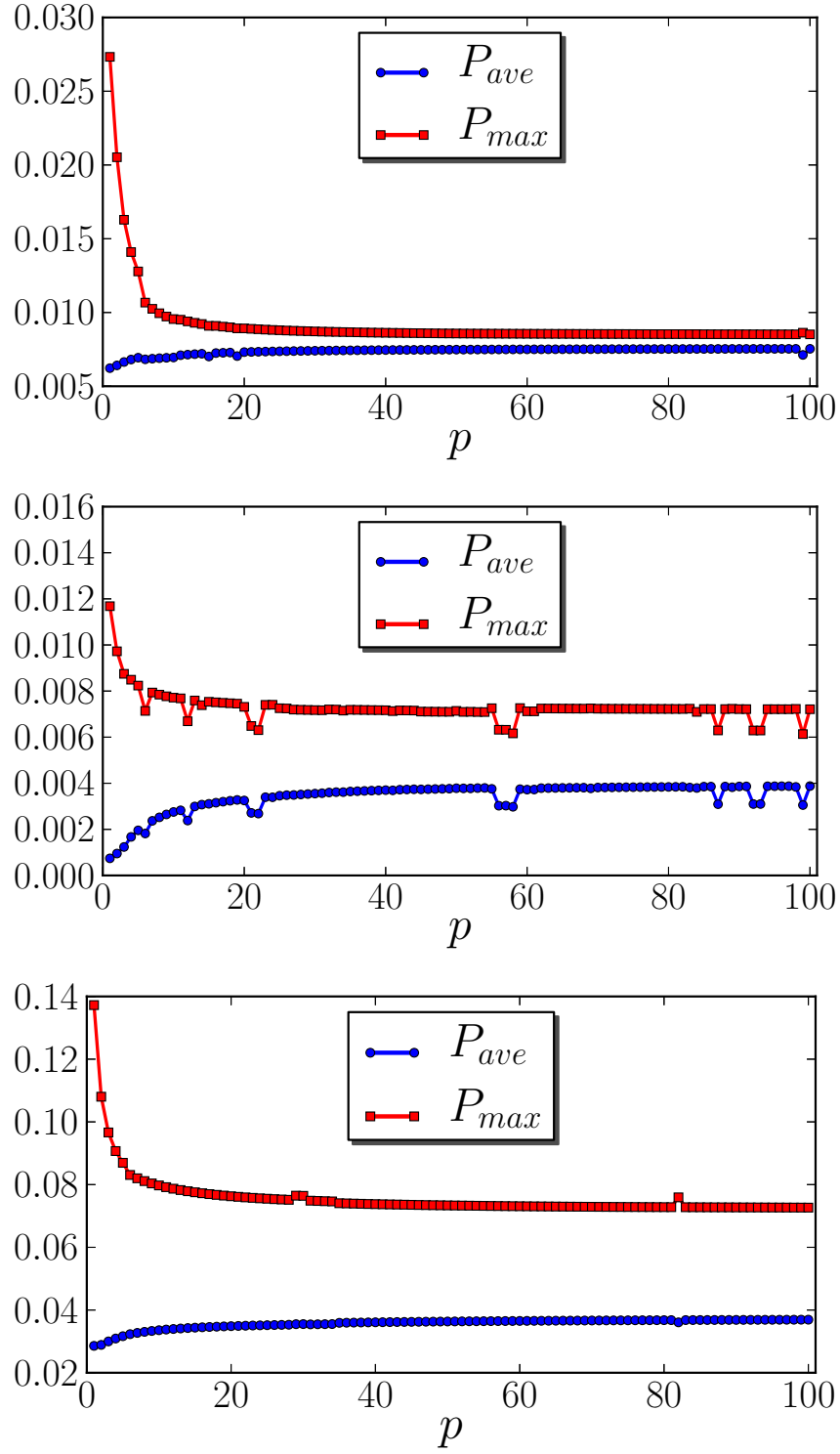
26

Figure 3.1: (For interpretation of the references to color in this and all other figures, the reader is referred to the electronic version of this dissertation.) Dependence of the average and maximal power reflectance on the norm of objective functions for three types of AR coatings. Top to bottom: broadband, omnidirectional and broadband-and-omnidirectional.

- The two values becomes rather close at large p in the broadband case but not the other two. This implies the power of reflection will be more evenly spread over the region of interest in the broadband case than the other two (compare Figures 3.3-3.5).

- The best achievable average and maximal power of reflection are much higher (10 times) in the broadband-and-omnidirectional case than the other two.

- There exist specific values of p at which both values experience abrupt changes in the omnidirectional case. However, this phenomenon is less evident in the broadband and broadband-and-omnidirectional cases. We believe it is because the merit functions are smoother in these cases but do not have a theoretical or numerical proof.

The last observation worthies more investigation since it is not as expected as the others. First we would like to point out the abrupt changes are not caused by the consolidation process. Our other experiments show they exist even if consolidations are not performed, although at possibly different values of p. At first glance it is against the intuition since the dependence of f_p on p is smooth. A small change in p can cause only a small change in f_p. However, f_p usually possess a large number of minima and our algorithms are local, so a small change in f_p could drive the solution to a different local minimum. For example, the two values experience abrupt changes from $p = 98$ to $p = 99$ and back to their normal values at $p = 100$. Figure 3.2 shows the refractive-index profiles and distribution of reflected power at $p = 98, 99$.

Comparing these with the result at $p = 100$ in Figure 3.4 reveals that the solutions at $p = 98, 100$ are the same local minimum but the solution at $p = 99$ is a different one. The existence of these different solutions at specific values of p is a good thing for coating designers. This is because one solution may be less sensitive to manufacture errors, possesses
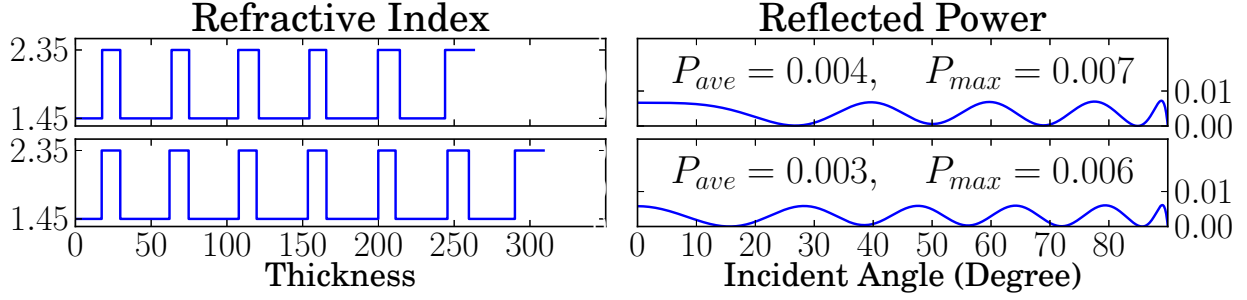
28

Figure 3.2: Refractive-index profiles and power of reflection in the omnidirectional case for $p = 98$ (top) and $p = 99$ (bottom).

better mechanical properties, or be easier to produce than another depending on the available deposition technology [35]. For example, the solution at $p = 99$ can be considered better than those at $p = 98$ and $p = 100$ due to its better optical performance and absence of thin layers.

Figures 3.3-3.5 show the refractive-index profiles and power of reflection at $p = 1, 100$ and ∞. Clearly the power distribution becomes more evenly spread as p increases in all three cases, confirming the statements in [20]. The solutions for $p = 100$ and $p = \infty$ could be very close, as in the broadband and broadband-and-omnidirectional cases, or rather different, as in the omnidirectional case, where the solution at $p = \infty$ contains much less layers and has a small decrease in performance than the solution at $p = 100$. This can be explained by the existence of neighboring local minima and the the use of different algorithms. Hence it is worthwhile to study the $p = \infty$ case since it may lead to different, possibly better solutions than finite values.

3.3 Conclusion

We have studied the problem of designing AR coatings by numerical optimization methods with different metrics. The merit functions in our approach are discrete approximations of

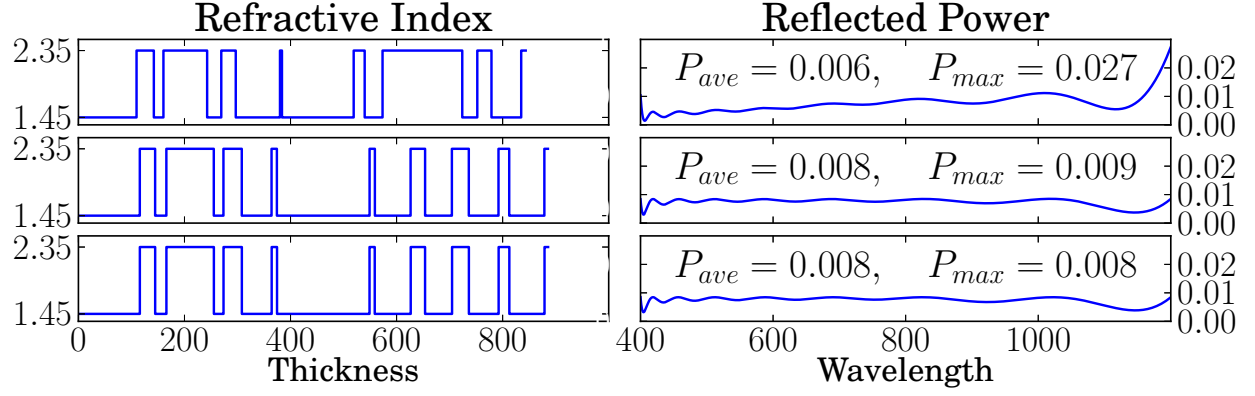Figure 3.3: Refractive-index profiles and reflected power for the broadband case at $p = 1, 100$ and $p = \infty$ (top to bottom).
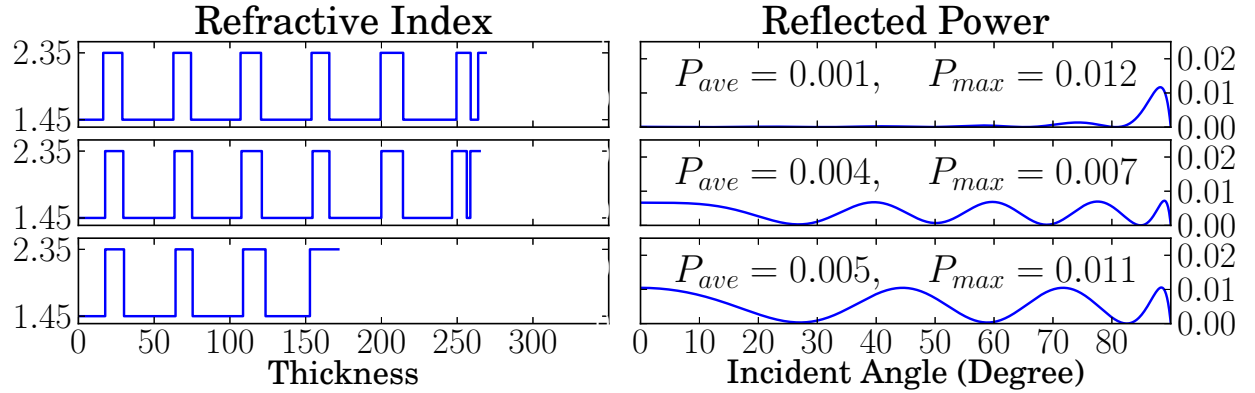

Figure 3.4: Refractive-index profiles and reflected power for the omnidirectional case at $p = 1, 100$ and $p = \infty$ (top to bottom).
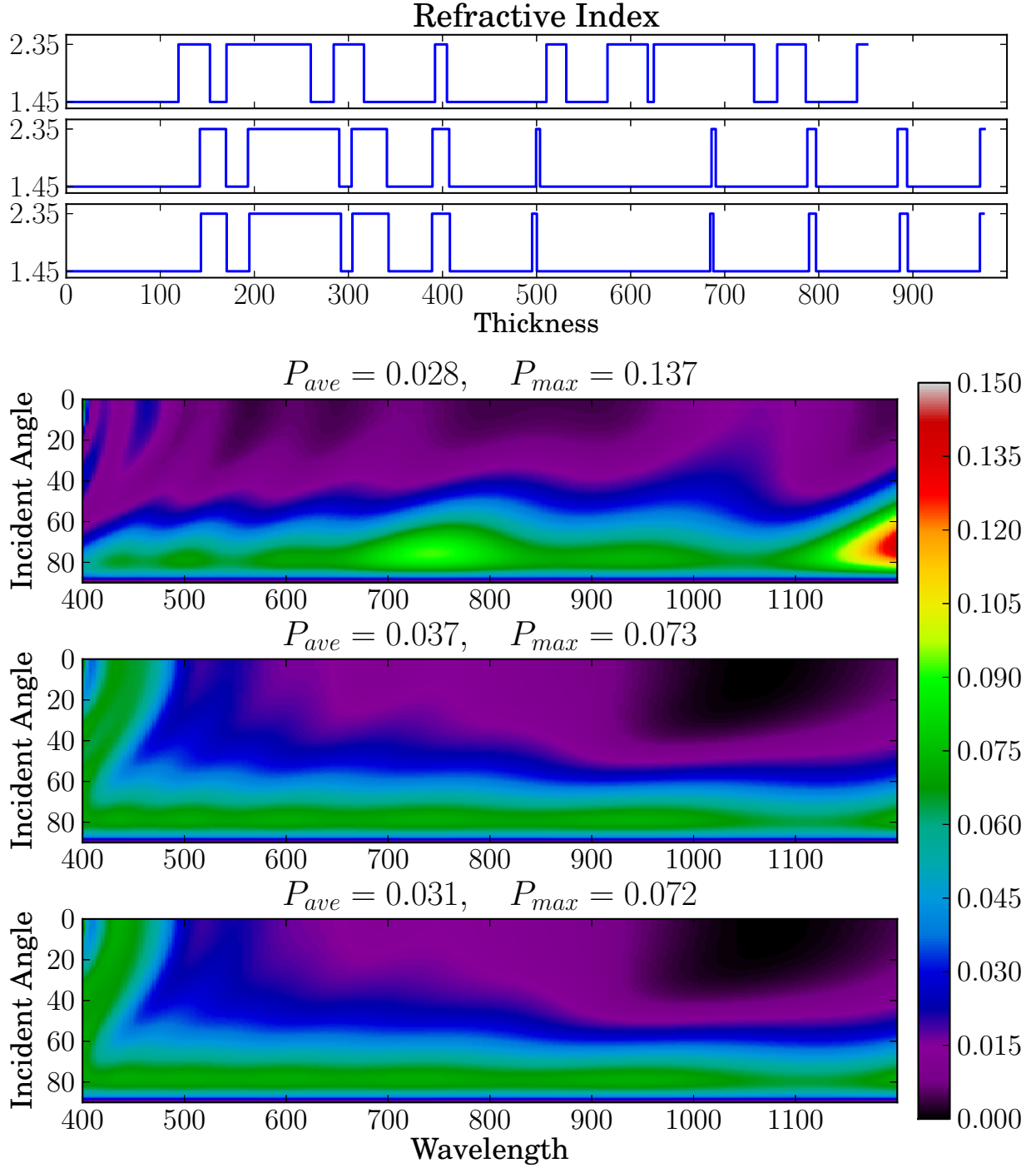
Figure 3.5: Refractive-index profiles and reflected power for the broadband-and-omnidirectional case at $p = 1, 100$ and $p = \infty$ (top to bottom).

the L^p norm of the reflected power over the region of interest. The impact of p on the optimal solutions are investigated by comparing the average and maximal power of reflection, which are important factors for practical applications. Based on our numerical experiments with three types of AR coatings, one should set p to 1 if one wishes to minimize the average value and to ∞ or a large value (e.g. 100) if one wishes to minimize the maximal value. Moreover, abrupt changes to the solutions can happen at specific values of p. This provides coating designers new opportunities in the search of better solutions.

Finally we would like to point out that the observed effect of metrics on the objective functions are not limited to multilayers or AR coatings. Similar effects are observed for rugates and other types of coatings during our numerical investigations.

Chapter 4

Rugate Coatings

Rugate coatings have been studied actively by scientists and engineers for more than 50 years. They have received considerable attention recently due to their outstanding optical, physical and feasibility properties.

4.1   Introduction

Based on the shape of the refractive-index profile, thin-film optical coatings are generally divided into two categories: multilayer coatings and rugate coatings. A multilayer coating consists of a stack of limited number of homogeneous layers. The refractive-index profile of such a coating is a step function taking a few number of fixed values. The most common coatings of this type are two-component multilayers, which consist of two materials. Rugate coatings were initially defined as optical coatings whose refractive-index profiles are constructed from sine and other known functions with explicit expressions. Now they are usually referred as optical coatings presenting any continuous refractive-index profiles. In this respect the term "rugate" may be used interchangeably with "gradient-index" or "inhomogeneous". Figure 4.1 shows the geometry for rugate coatings.

Since a continuous function can be approximated by step functions up to any given accuracy and the practical computation of rugate coatings are commonly conducted through subdivision of the film into a large number of homogeneous layers, the boundaries that
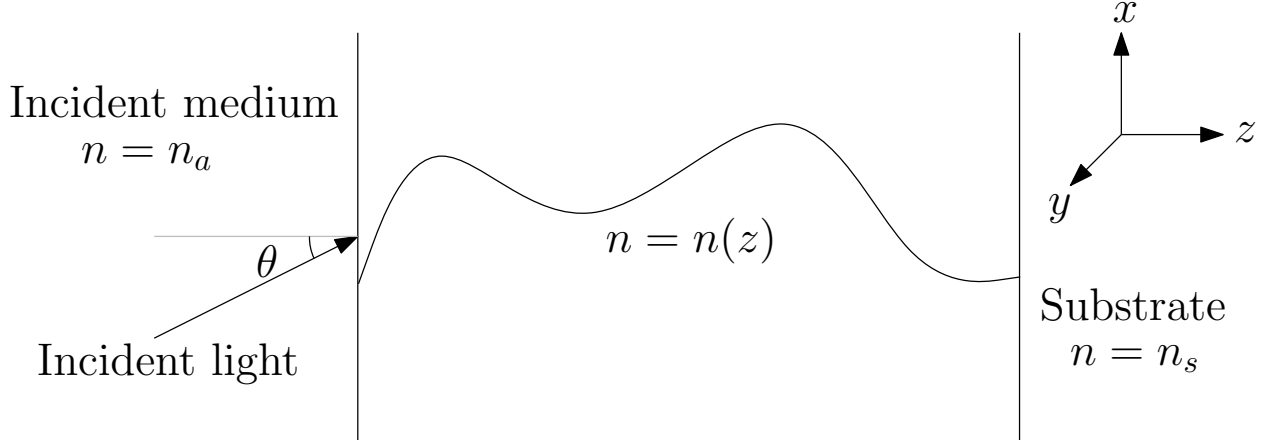
Figure 4.1: Problem geometry for rugate coatings.

define multilayer and rugate coatings can become unclear. Those in the intermediate region can be called quasi-rugate coatings, which include multilayers with intermediate refractive indices, two-component multilayers with a large number of layers, and coatings possessing both homogeneous and inhomogeneous layers.

Multilayer coatings have been successfully designed and produced to fulfill a wide range of desired optical properties. But it is still desirable to study rugate coatings because they are advantageous to multilayers in three aspects [36, 35]. Firstly, rugate coatings can have better optical properties. In the case of nonabsorbing dielectric coatings at s-polarization or p-polarization at small incident angles, the maximum principle of thin-film optics [6] predicts that the optimal refractive-index profile is a step function taking the lowest and highest permissible values, i.e. the optimal design is a two-component multilayer. However, the conclusion of this principle becomes unclear or invalid if the coating materials are absorbing, or if the design target is specified at wide incident angles and/or both polarization. Under those circumstances the rugate and quasi-rugate coatings can have superior optical performance comparing with multilayers. Secondly, rugate coatings can have better feasibility properties. Some multilayer designs are very sensitive to manufacturing errors, especially

when there are many thin layers and the total number of layers is large. It has been demonstrated experimentally that many rugate coatings possess better feasibility properties than their multilayer correspondence. Thirdly, rugate coatings have better physical properties, including mechanical and thermal stability.

The Fourier transform method [37] is a powerful and widely used method for the design of rugate coatings. It is based on the approximate expression:

$$\frac{1}{2} \int_{-\infty}^{\infty} [\ln n(x)]' e^{ikx} dx = Q(k) e^{i\phi(k)}$$

where

- $n(x)$ is the refractive-index profile

- $Q(k)$ is an suitable even function of the target transmittance $T(k)$

- $\phi(k)$ is an odd function to ensure $n(x)$ is real (Note: $\phi(k)$ is NOT the phase change of reflection or transmission)

- x is twice the optical thickness: $x = 2 \int_0^z n(s) ds$

- k is the wavenumber: $k = 2\pi/\lambda$

The Fourier transform method is very fast when it works. However it has the following disadvantages and limitations:

- based on approximate equations assuming the following conditions

  - low reflection

  - no absorption (real refractive index)

– no dispersion (refractive index is independent of wavelength)

- infinitely thick coating

- difficult to implement constraints on the refractive index

- can not handle the cases when more than one incident angle or polarization is specified

- can not handle phase specifications

4.2   Smooth by Penalty Terms

Straightforward optimization of the merit functions $\|R(n,k) - \tilde{R}(k)\|$ will lead to solutions which resemble multilayers or contain many discontinuities. One method to force smoothness of the solutions is by adding penalty terms. This is the approach adopted in [21], where the the refractive-index profile $n(z)$ is parameterized as polylines $\{(z_i, n_i) : 1 \leq i \leq N\}$ and the objective function is defined as

$$f(X) = \frac{1}{L} \sum_{j=1}^{L} \left[\frac{R(X, \lambda_j) - \tilde{R}(\lambda_j)}{\Delta_j} \right]^2 + \alpha \sum_{j=1}^{N-1} \left(\frac{n_{j+1} - n_j}{z_{j+1} - z_j} \right)^2.$$

where $X = (z_1, \cdots, z_N, n_1, \cdots, n_N)$. Our approach is similar except $n(z)$ is parameterized as step functions $\{(t_i, n_i) : 1 \leq i \leq N\}$ and use of different metrics in the objective functions:

$$f(X) = \left\{ \frac{1}{L} \sum_{j=1}^{L} \left[\frac{R(X, k_j) - \tilde{R}(k_j)}{\Delta_j} \right]^p \right\}^{\frac{1}{p}} + \alpha \left\{ \frac{1}{N-1} \sum_{j=1}^{N-1} \left[\frac{2(n_{j+1} - n_j)}{t_i + t_{i+1}} \right]^q \right\}^{\frac{1}{q}}.$$

where p, q are even natural numbers (p can be odd if $\tilde{R}(k_j) \equiv 0$), Δ_j are design tolerances and α is a weight factor controlling balance between the performance and smoothness of the
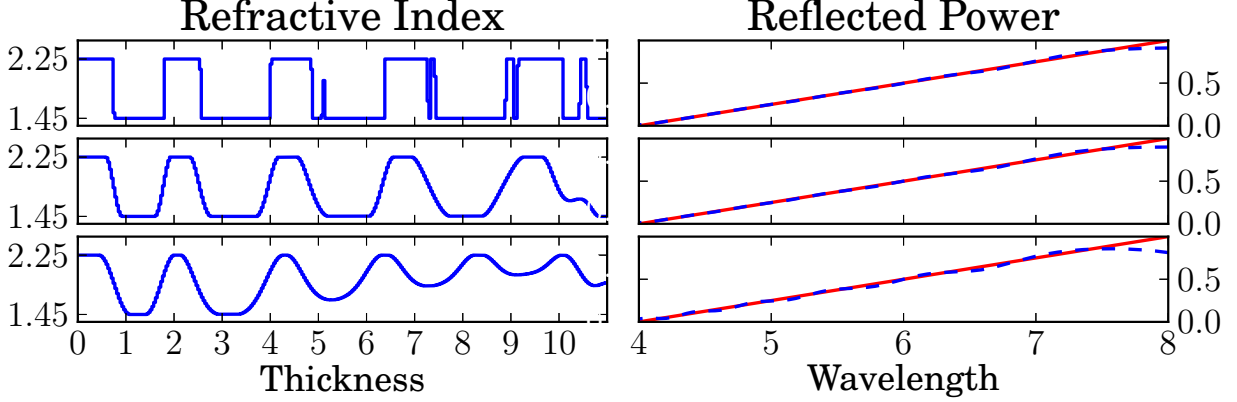
Figure 4.2: Refractive-index profiles (left) and reflectance curves (right) of optimal solutions for a ramp filter. Top to bottom: $\alpha = 0, 0.01, 0.1$.

resultant refractive-index profiles. Notice that the penalty term is a discretization of the L^q norm of the $n'(z)$. The gradient of $f(X)$ can be computed easily using the derivative formulas for R derived in chapter 1.

My approach differs from [21] in three aspects. First, $n(z)$ is parameterized by step functions instead of polylines. Using step functions simplifies the calculation and the results are similar to those using polylines. Second, effect of different metrics in both the merit (controlled by p) and penalty functions (controlled by q) will be investigated. In particular, the use of high values for q yield interesting solutions never seen before. Third, the penalty term is normalized with respect to the number of parameters so that the choice of the value for α will be independent of the level of discretization.

Figure 4.2 shows the refractive-index profiles (left) and reflectance curves (right) of optimal solutions for a ramp filter with different values of α. We have set $p = q = 2$ in this test. Observe how the refractive-index profile becomes smoother as α increases. As expected, the performance deteriorates as α increases. Remarkably, a small value of α can smooth the solution effectively with little effect on the performance.

The effect of p on the solutions are similar to multilayer cases as explained in the previous
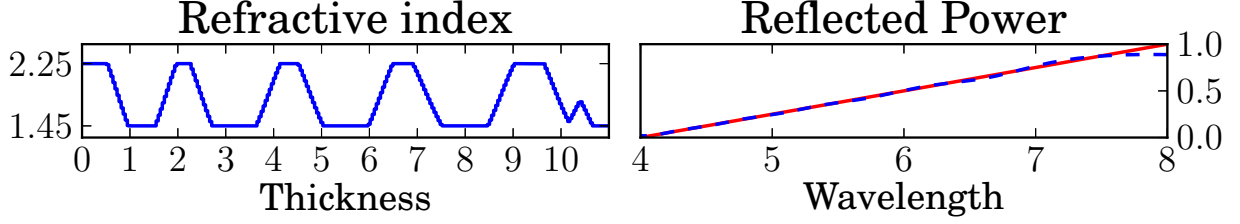
Figure 4.3: Refractive-index profile (left) and reflectance curve (right) of the optimal solution for a ramp filter with $\alpha = 0.01, p = 2, q = 10$.
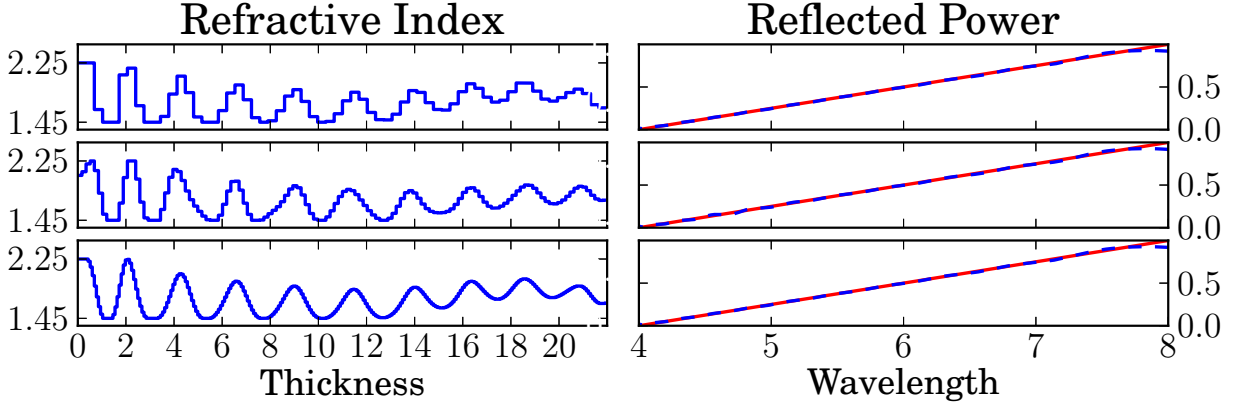
Figure 4.4: Dependence of the solution on N. Top to bottom: $N = 64, 128, 256$.

section. The effect of q is more interesting.

Figure 4.3 shows the solutions of the same problem but with $\alpha = 0.01$ and $q = 10$. Notice the solution is qualitatively similar to the $q = 2$ but the curved parts are straightened up. On the other hand, the difference in performance is negligible. Again, this is beneficial since different solutions are always desirable.

Next we investigate the impact of the level of discretization on the performance of the design. In principle, the finer the discretization the better performance is expected since we have more degrees of freedom. In practice, however, the impact becomes negligible at rather rough discretization. Figure 4.4 shows the refractive-index profiles and the corresponding reflectance curves for the same problem but with different level of discretization. Notice the performance of these designs are almost indistinguishable from each other although the

refractive-index profiles are very different. There are two heuristic explanations for this phenomenon. First, it is a well known fact that small features of a structure has little effect on waves with large wavelength. Thus refinement of the refractive-index in fine scale has little impact on its optical performance. This is confirmed from the numerical results, where we see the refractive-index profiles obtained with finer discretization are generally the interpolations of those obtained with rough discretization. Second, the number of local minima increases fast as the number of variables increases. So it is more likely to get stuck in a bad local minimum with finer discretization.

We are motivated by the fact that the refractive-index profiles obtained with finer discretization are generally the interpolations of those obtained with rough discretization and devised a method to speed up the convergence:

1. set N to a small number, e.g. 8

2. optimize until convergence is reached

3. divide each layer into two sub-layers of equal thickness

4. set refractive index of the sub-layers by interpolation from neighbor layers

5. go to step 2 and repeat until desired number of layers is reached

This simple algorithm can increase convergence speed about three fold for most experiments we conducted. Further improvements are achieved if we increase the convergence tolerance progressively in step 2.

Chapter 5

Global Basis Functions

Existing optimization methods for the optimal design of thin-film coatings have used only local basis functions (step and hat functions) for the parameterization of the refractive-index profile. Global basis functions such as sinusoidal functions have been used only in heuristic design methods, where there are only a few design parameters such as the amplitude, frequency and shifting. The coatings that can be designed by heuristic methods are very limited.

The Fourier transform method finds the refractive-index profiles as an inverse Fourier transform of an appropriate function. However, it is not an optimization method and has many limitations.

5.1 Formulation

The problem of using global basis functions is that there is no direct way to translate the bound constraints on the refractive-index profile to its spectral coefficients. This is also the major difficulty and limitation of the Fourier transform method.

To overcome this difficulty, we transform the set of bounded functions $\{n(z) \in L^\infty(0, L) : n_L \leq n(z) \leq n_H\}$ to the set of unbounded functions $\{m(z) : m(z) \in L^\infty(0, L)\}$ through the

mapping

$$m(z) = \frac{w(n(z) - c)}{\sqrt{w^2 - (n(z) - c)^2}}, \tag{5.1}$$

where $w = (n_H - n_L)/2$ and $c = (n_H + n_L)/2$. This transformation is obtained by mapping the line segment (n_L, n_H) to $(-\infty, \infty)$ through a half circle. This mapping can be inverted to get an expression of $n(z)$ in terms of $m(z)$:

$$n(z) = c + \frac{wm(z)}{\sqrt{m(z)^2 + w^2}}. \tag{5.2}$$

This particular choice of mapping is picked by intuition and is not necessarily the best. In fact, there are infinitely many choices out there, e.g. the tangent function

$$m(z) = \tan\left(\frac{\pi}{w}(x - c)\right).$$

Now there is no bound constraints on $m(z)$, let us approximate it by truncated Fourier series

$$m(z) \approx \sum_{j=0}^{N} a_j \cos\left(\frac{j\pi}{L}x\right) + \sum_{j=1}^{N} b_j \sin\left(\frac{j\pi}{L}x\right). \tag{5.3}$$

It is certainly possible to use other global basis functions such as Chebyshev or Hermite polynomials.

Given a vector of coefficients $\{a_0, \cdots, a_N, b_1, \cdots, b_N\}$ we have a function $m(z)$ from (5.3) and a refractive-index profile $n(z)$ by solving (5.1). The reflectance curve corresponding to $n(z)$ can be then computed from the matrix method. Thus we have a function mapping the Fourier coefficients to reflectance and the unconstrained optimization problem for a

broadband coating:

$$\min_{a_0,\cdots,a_N,b_1,\cdots,b_N} \|R(k; a_0,\cdots,a_N, b_1,\cdots,b_N) - \tilde{R}(k)\|_{L^p(k_L,k_H)}, \tag{5.4}$$

where $R(k; a_0,\cdots,a_N, b_1,\cdots,b_N)$ is the reflectance at wavenumber k of a refractive-index profile $n(z)$ obtained from the coefficients $\{a_0,\cdots,a_N, b_1,\cdots,b_N\}$ and $\tilde{R}(k)$ is the target reflectance function.

To compute the reflectance and its gradient, we discretize $n(z)$ and $m(z)$ by piece-wise constant functions. Divide the coating into D sub-layers of equal thickness. Denote z_i the center of the $i-th$ layer and $n_i = n(z_i), m_i = m(z_i)$, Then the reflectance R is computed from the matrix method and the partial derivatives of R is given by

$$\frac{\partial R}{\partial a_j} = \sum_{i=1}^{D} \frac{\partial R}{\partial n_i} \frac{\partial n_i}{\partial m_i} \frac{\partial m_i}{\partial a_j} \tag{5.5a}$$

$$= \sum_{i=1}^{D} \frac{\partial R}{\partial n_i} w^3 (m_i^2 + w^2)^{-\frac{3}{2}} \cos\left(\frac{j\pi}{L} z_i\right), \ 0 \leq j \leq N, \tag{5.5b}$$

$$\frac{\partial R}{\partial b_j} = \sum_{i=1}^{D} \frac{\partial R}{\partial n_i} \frac{\partial n_i}{\partial m_i} \frac{\partial m_i}{\partial a_j} \tag{5.5c}$$

$$= \sum_{i=1}^{D} \frac{\partial R}{\partial n_i} w^3 (m_i^2 + w^2)^{-\frac{3}{2}} \sin\left(\frac{j\pi}{L} z_i\right), \ 1 \leq j \leq N, \tag{5.5d}$$

where $\partial R/\partial n_i$ is also computed from the matrix method.

5.2 Numerical Experiments

Consider a broadband antireflection coating over the wavelength range $[\lambda_L, \lambda_H] = [400, 1200]$ at TE polarization and normal incident angle. The refractive indices of the incident medium
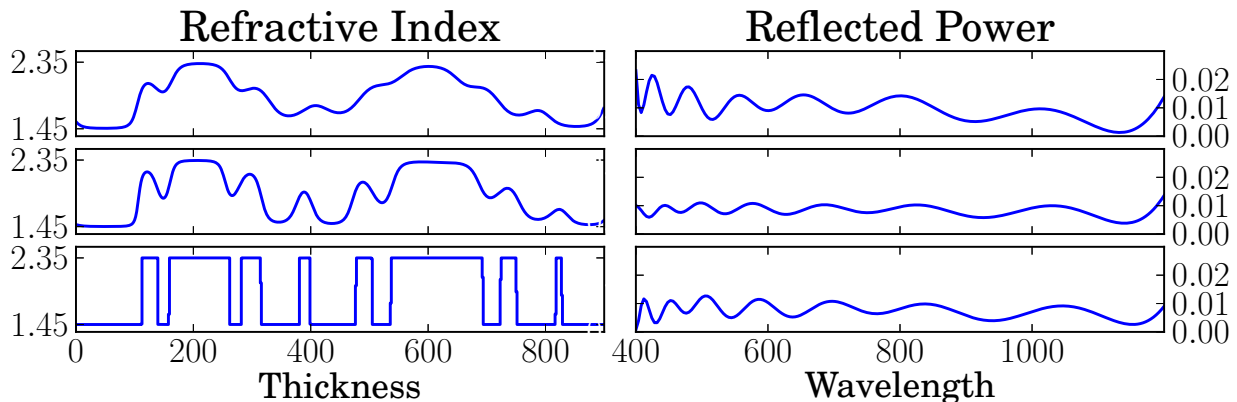
Figure 5.1: Snapshots of the refractive-index profile (left) and reflectance (right) at 10, 50, and 200 iterations (top to bottom) during the optimization of a broadband AR coating parameterized by sinusoidal functions.

and substrate are $n_a = 1.0$ and $n_s = 1.52$ respectively. The lower and upper bound of the refractive index of the coating is $n_L = 1.45$ and $n_H = 2.35$ respectively. The total thickness of the coating is $L = 900$. The number of terms in the Fourier series is $N = 20$ and the initial guess is $\{a_0, \cdots, a_N, b_1, \cdots, b_N\} = \{1, \cdots, 0, 0, \cdots, 0\}$, corresponding to $m(z) = 1$ and $n(z) = (n_L + n_H)/2$. The Matlab function "fmincon" is used to run the optimization. Figure 5.1 shows the snapshots of the refractive-index profile $n(z)$ and the corresponding reflectance curves $R(\lambda)$ at 10, 50, and 200 iteration steps during the optimization.

We have a number of observations from this example.

First, it is interesting to see how $n(z)$ evolves from a smooth function to an almost-step function taking only two values, namely the lower and upper bounds n_L, n_H. This is consistent with the maximum principle of thin-film optics [38].

Second, $n(z)$ varies much more significant than $R(\lambda)$ does during the iterations. This is due to the ill-posedness of the corresponding inverse problem of recovering $n(z)$ from $R(\lambda)$. While ill-posedness is generally considered to be a disadvantage of inverse problems, it is the opposite in this case since we can have very different designs with similar performance.

For example, the rugate (2nd) and multilayer (3rd) designs in Figure 5.1 are qualitatively different but their performance are almost identical.

Third, the reflectance curves are uniformly distributed in the spectral region even if $p = 1$ is used in the objective function (5.4). In contrast, the reflectance curves obtained by using local basis functions with small values of p possess a peak at the upper bound of the spectral region.

Ongoing and future works in this topic include the possibilities to use other transformations and basis functions, determine the appropriate value for the number of terms N or how to increase it progressively to obtain better solutions or increase convergence speed. We shall also consider the use of penalty or constraint functions to force smoothness of $n(z)$ as we did in chapter 4.

Chapter 6

Diffraction Gratings

So far we considered only optical coatings built from layer structures. The refractive index of such structures vary along one direction and is homogeneous over the other two. By allowing the refractive index of the structure to vary periodically along one or both of the other two directions one obtains singly or doubly periodic structures, often called 2D or 3D diffraction gratings, respectively. Dobson studied the optimal design of wide-angle antireflective diffraction gratings [7] and blazed diffraction gratings [8]. Following the spirit of these work, we study the optimal design of broadband optical coatings by the use of diffraction gratings. The value and gradient of the objective function will be obtained by solving a 2D PDE with nonlocal transparent boundary conditions [9] and the corresponding adjoint equation [7], respectively.

6.1   Model and Forward Solver

Consider a 1D diffraction grating so that $\mu = 1$ and ε is invariant along y-axis with

$$
\varepsilon(x, z) = \begin{cases} \varepsilon_1, & z \geq b - \delta, \\ \varepsilon(x + \Lambda, z), & -b + \delta < z < b - \delta, \\ \varepsilon_2, & z \leq -b + \delta \end{cases}
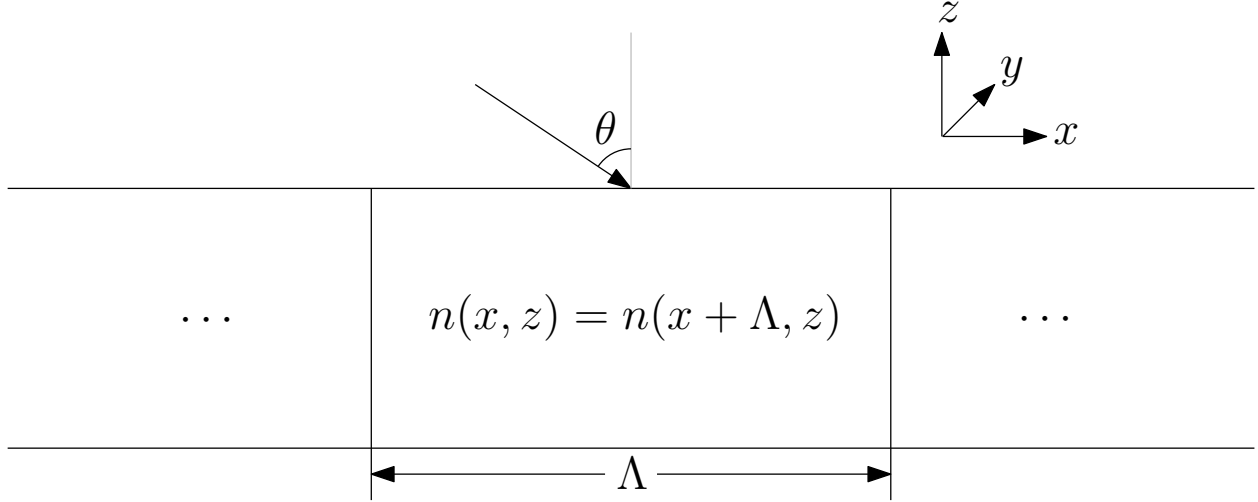$$

Figure 6.1: Problem geometry for 1D diffraction gratings.

where $b > 0, \delta > 0$ are a constants with $b - \delta > 0$. Figure 6.1 summarizes the geometry for 1D diffraction gratings.

Given a time harmonic plane incident wave, we will determine the reflectance and transmittance by the variational approach with transparent boundary conditions [9]. The Maxwell's equations for a time harmonic wave with frequency ω reduce to the following coupled system of linear equations

$$\nabla \times \mathbf{E} - ik\mathbf{H} = 0, \tag{6.1a}$$

$$\nabla \times \mathbf{H} + ik\varepsilon\mathbf{E} = 0, \tag{6.1b}$$

where $k = \omega/c$ is the wavenumber in vacuum. We also have the following boundary conditions at a surface of discontinuity:

$$\mathbf{n_{12}} \times (\mathbf{E_2} - \mathbf{E_1}) = 0, \tag{6.2a}$$

$$\mathbf{n_{12}} \times (\mathbf{H_2} - \mathbf{H_1}) = 0, \tag{6.2b}$$

46

In the case of TE polarization, the system of linear equations reduces to the Helmholtz equation

$$(\Delta + k^2 \varepsilon)u = 0,$$

where u is the tangential component of $\mathbf{E}$. For the sake of uniqueness, we only look for quasi periodic solutions u such that

$$u_\alpha = u \exp(-i\alpha x)$$

is Λ periodic, where $\alpha = k\varepsilon_1 \sin\theta$ and θ is the angle of incidence.

Denote

$$\Omega = \{(x, z) : -b < z < b\}, \tag{6.3a}$$

$$\Omega_1 = \{(x, z) : z \geq b\}, \tag{6.3b}$$

$$\Omega_2 = \{(x, z) : z \leq -b\}, \tag{6.3c}$$

$$\Gamma_1 = \{(x, z) : z = b\}, \tag{6.3d}$$

$$\Gamma_2 = \{(x, z) : z = -b\}. \tag{6.3e}$$

$$\tag{6.3f}$$

For each $n \in \mathbb{Z}$ denote $\alpha_n = 2\pi n/\Lambda$. By expanding u_α into its Fourier series along the x-axis:

$$u_\alpha(x, z) = \sum_{n \in \mathbb{Z}} u_\alpha^{(n)}(z) \exp(i\alpha_n x), \tag{6.4a}$$

$$u_\alpha^{(n)}(z) = \frac{1}{\Lambda} \int_0^\Lambda u_\alpha(x, z) \exp(-i\alpha_n x) dx, \tag{6.4b}$$

the fact that u_α is a sum of plane waves in Ω_1, Ω_2:

$$u_\alpha(x, z)|_{\Omega_j} = \sum_{n \in \mathbb{Z}} a_j^{(n)} \exp[\pm i\beta_j^{(n)} z + i\alpha_n x], \tag{6.5}$$

and the continuity of u and $\partial u/\partial \nu$ across Γ_1, Γ_2, we obtain the following boundary value problem for u_α

$$(\Delta_\alpha + k^2 \varepsilon)u = 0, \text{ in } \Omega, \tag{6.6a}$$

$$(\frac{\partial}{\partial \nu} - T_1)u_\alpha = -2i\beta \exp(-i\beta b), \text{ on } \Gamma_1, \tag{6.6b}$$

$$(\frac{\partial}{\partial \nu} - T_2)u_\alpha = 0, \text{ on } \Gamma_2, \tag{6.6c}$$

where

$$\Delta_\alpha = \Delta + 2i\alpha\partial_x - |\alpha|^2,$$

$$T_j f = \sum_{n \in \mathbb{Z}} i\beta_j^{(n)} f^{(n)} \exp(i\alpha_n x),$$

$$f^{(n)} = \frac{1}{\Lambda} \int_0^\Lambda f(x) \exp(-i\alpha_n x)dx, \tag{6.7}$$

$$\beta_j^{(n)} = \sqrt{k^2 \varepsilon_j - (\alpha_n + \alpha)^2} \quad \text{s.t. } \arg(\beta_j^{(n)}) \in [0, \pi),$$

$$\beta = k\varepsilon_1 \cos\theta$$

Here and in the sequel the domain and boundary will be restricted into one periodic cell $\{(x, z) : 0 < x < \Lambda\}$.

Denote $H(\Omega) = \{v : v \in H^1(\Omega), v(0) = v(L)\}$ where $H^1(\Omega)$ is the standard Sobolev space. Multiplying the PDE in (6.6a) by the conjugate of a test function $\phi \in H(\Omega)$ and applying Green's formula with the given boundary conditions, we obtain the variational, or

48

weak, formulation of the boundary value problem (6.6a):

$$
\begin{aligned}
&- \int_\Omega \nabla u_\alpha \cdot \nabla \overline{\phi} + \int_\Omega (k^2 \varepsilon - \alpha^2) u_\alpha \overline{\phi} + 2i\alpha \int_\Omega (\partial_x u_\alpha) \overline{\phi} \\
&+ \int_{\Gamma_1} (T_1 u_\alpha) \overline{\phi} + \int_{\Gamma_2} (T_2 u_\alpha) \overline{\phi} \\
&= 2i\beta \int_{\Gamma_1} \exp(-i\beta b) \overline{\phi}.
\end{aligned}
$$

This variational formulation will be discretized and solved by the finite element method.

The layered structures studied in the previous chapters have the property that the reflected light propagates in a single direction, so is the transmitted light. On the other hand, diffraction gratings can have light reflected and transmitted in multiple directions. This can be seen from (6.5) and the definition of $\beta_j^{(n)}$ in (6.7). Each real value of $\beta_j^{(n)}$ corresponds to a propagating mode and each complex value corresponds to an evanescent mode (propagates along the x-axis and decreases exponentially along z-axis).

For real values of $\epsilon_j, j = 1, 2$, the set of values of n such that $\beta_j^{(n)}$ is real is given by

$$
\Lambda_j = \{ n \in \mathbb{Z} : |\alpha_n + \alpha| < k^2 \varepsilon_j \}. \tag{6.8}
$$

Once the solution u_α is obtained, we can determine for each order $n \in \Lambda_j$ the amplitude reflectance r_n and amplitude transmittance t_n from (6.4a) and (6.5):

$$
r_0 = u_\alpha^{(0)}(b) \exp(-i\beta_1^{(0)} b) - \exp(-2i\beta_1^{(0)} b), \tag{6.9a}
$$

$$
r_n = u_\alpha^{(n)}(b) \exp(-i\beta_1^{(n)} b), \quad n \in \Lambda_1, \tag{6.9b}
$$

$$
t_n = u_\alpha^{(n)}(-b) \exp(-i\beta_2^{(n)} b), \quad n \in \Lambda_2. \tag{6.9c}
$$

As for the layered structures, we then use Poynting vector to determine the corresponding power reflectance R_n and power transmittance T_n and obtain the following:

$$R_n = |r_n|^2 \frac{\cos \theta_1^{(n)}}{\cos \theta}, \tag{6.10a}$$

$$T_n = |t_n|^2 \frac{\cos \theta_2^{(n)}}{\cos \theta} \sqrt{\frac{\varepsilon_2}{\varepsilon_1}}, \tag{6.10b}$$

$$\tag{6.10c}$$

where $\theta_j^{(n)}, j = 1, 2$ is the angle of propagation for mode of order n and is given by

$$\theta_j^{(n)} = \arctan \left(\frac{\alpha_n + \alpha}{\beta_j^{(n)}} \right).$$

6.2 Adjoint Problem and Gradient

As in the layered structures, we need to find a method to compute the gradient of the reflectance and transmittance if we would like to use gradient based optimization algorithms. Unlike the layered structures, we do not have a explicit expression relating the reflectance R_n to the permittivity ε. We derive the formula for the gradient by extending the formal argument as in [7].

Let ε be fixed and $\delta \varepsilon$ be a small perturbation. By (6.4a) and (6.9a) we obtain the directional derivative

$$D_\varepsilon r_n(\delta \varepsilon) = k^2 \frac{\exp(-i\beta_1^{(n)}b)}{\Lambda} \int_{\Gamma_1} \delta u_\alpha \exp(-i\alpha_n x) dx, \tag{6.11}$$

where δu_α is the solution for the following boundary value problem:

$$(\Delta_\alpha + k^2 \varepsilon)\delta u_\alpha = -k^2 \delta \varepsilon u_\alpha, \tag{6.12a}$$

$$\left(T_j - \frac{\partial}{\partial \nu}\right)\delta u_\alpha|_{\Gamma_j} = 0, \quad j = 1, 2. \tag{6.12b}$$

Let w_α be the solution of the following "adjoint problem":

$$(\Delta_\alpha + k^2 \bar{\varepsilon})w_\alpha = 0, \tag{6.13a}$$

$$\left(T_1^* - \frac{\partial}{\partial \nu}\right)w_\alpha|_{\Gamma_1} = -\phi(x), \tag{6.13b}$$

$$\left(T_2^* - \frac{\partial}{\partial \nu}\right)w_\alpha|_{\Gamma_2} = 0, \tag{6.13c}$$

$$\tag{6.13d}$$

where $\phi(x) = r_n \exp(i\alpha_n x)$ and

$$T_j^* f = \sum_{n \in \mathbb{N}} -i\overline{\beta_j^{(n)}} f^{(n)} \exp(i\alpha_n x).$$

Multiplying the first equation in (6.12a) by $\overline{w_\alpha}$ and applying Green's formula yields

$$\int_\Omega \delta \varepsilon u_\alpha \overline{w_\alpha} = \int_{\Gamma_1} \delta u_\alpha \overline{\phi}$$

$$= \overline{r_n} \int_{\Gamma_1} \delta u_\alpha \exp(-i\alpha_n x) \tag{6.14}$$

$$= \frac{\Lambda}{k^2 \exp(-i\beta_1^{(n)})b} \overline{r_n} D_\varepsilon r_n(\delta \varepsilon).$$

Hence

$$D_\varepsilon R_n(\delta \varepsilon) = 2k^2 \frac{\exp(-i\beta_1^{(n)})b}{\Lambda} \int_\Omega \delta \varepsilon u_\alpha \overline{w_\alpha}. \tag{6.15}$$

This implies the L^2-gradient of R_n with respect to ε is given by

$$\nabla_\varepsilon R_n = \overline{2k^2 \frac{\exp(-i\beta_1^{(n)})b}{\Lambda} \int_\Omega u_\alpha \overline{w_\alpha}} = 2k^2 \frac{\exp(i\beta_1^{(n)})b}{\Lambda} \int_\Omega \overline{u_\alpha} w_\alpha, \qquad (6.16)$$

The expressions for $\nabla_\varepsilon T_n$ can be obtained in a similar fashion.

6.3   Numerical Experiments

In order to solve the optimization problem numerically, we need first discretize the functional space $L^\infty(\Omega)$ for ε. We are going to use finite element method with rectangular bilinear elements, so it is most natural here to discretize ε by piece-wise constant functions over rectangular mesh. For real ε we define

$$\varepsilon_{i,j} = \chi_{[(j-1)\Delta_x, j\Delta_x] \times [(i-1)\Delta_y, i\Delta_y]},$$

where χ is the standard characteristic function. For complex valued ε we can consider the real and imaginary parts separately. For the sake of convenience, the mesh size Δ_x, Δ_y are chosen to be integer multiples of the mesh size for the finite element space. By (6.16) we obtained the discrete version of the gradient

$$\nabla_{i,j} R_n = \Re \left\{ 2k^2 \frac{\exp(i\beta_1^{(n)})b}{\Lambda} \int_\Omega \overline{u_\alpha} w_\alpha \varepsilon_{i,j} \right\}. \qquad (6.17)$$

Let us consider the design of a diffraction grating with broadband antireflection proper-

ties. The objective function is a normalized discretization of $\|R_0\|_1$:

$$f(\epsilon) = \frac{1}{N} \sum_{i=1}^{N} R(\epsilon; k_i),$$

where $\epsilon = \{\varepsilon_{i,j}\}$ are design variables and $\{k_i\}$ is a uniform set of sampling points in the spectral region of interest.

The refractive indices of the incident medium and substrate are 1.0 and 1.52 respectively. The lower and upper bound of the refractive index of the coating are 1.45 and 2.35 respectively. We assume normal incidence and TE polarization. The range of wavelength is $[\lambda_L, \lambda_H] = [1, 3]$. The depth of the grating is $2b = 2$ and the period $\Lambda = 0.99\lambda_L\sqrt{\varepsilon_1}$. Notice this value of Λ will guarantee only the zero-th reflecting order is propagating so that only R_0 is nonzero for all wavelength by (6.8). By increasing Λ we will introduce more propagating orders and it is up to the user to minimize one of the orders or the combination of them.

The domain Ω is divided into 32×64 uniform rectangular mesh and ε is discretized by 16×32 uniform rectangular mesh. The minimization of the objective function is done by the "fmincon" command in Matlab, and the algorithm is chosen to be "active-set". The maximal iteration step is set to 300.

In the first experiment we choose the initial guess to be the homogeneous profile $\varepsilon = \sqrt{\varepsilon_1\varepsilon_2}$. Figure 6.2 shows the refractive-index profiles and reflectance curves for the initial guess and optimized solution. The refractive index is normalized from $[n_L, n_H]$ to $[0, 64]$ so that it can be represented as a gray scale image. This transformation is used in all the following figures.

A notable feature of the optimized profile it resembles a multilayer structure, i.e the refractive index in invariant along the x-axis and is mostly piece-wise constants along the
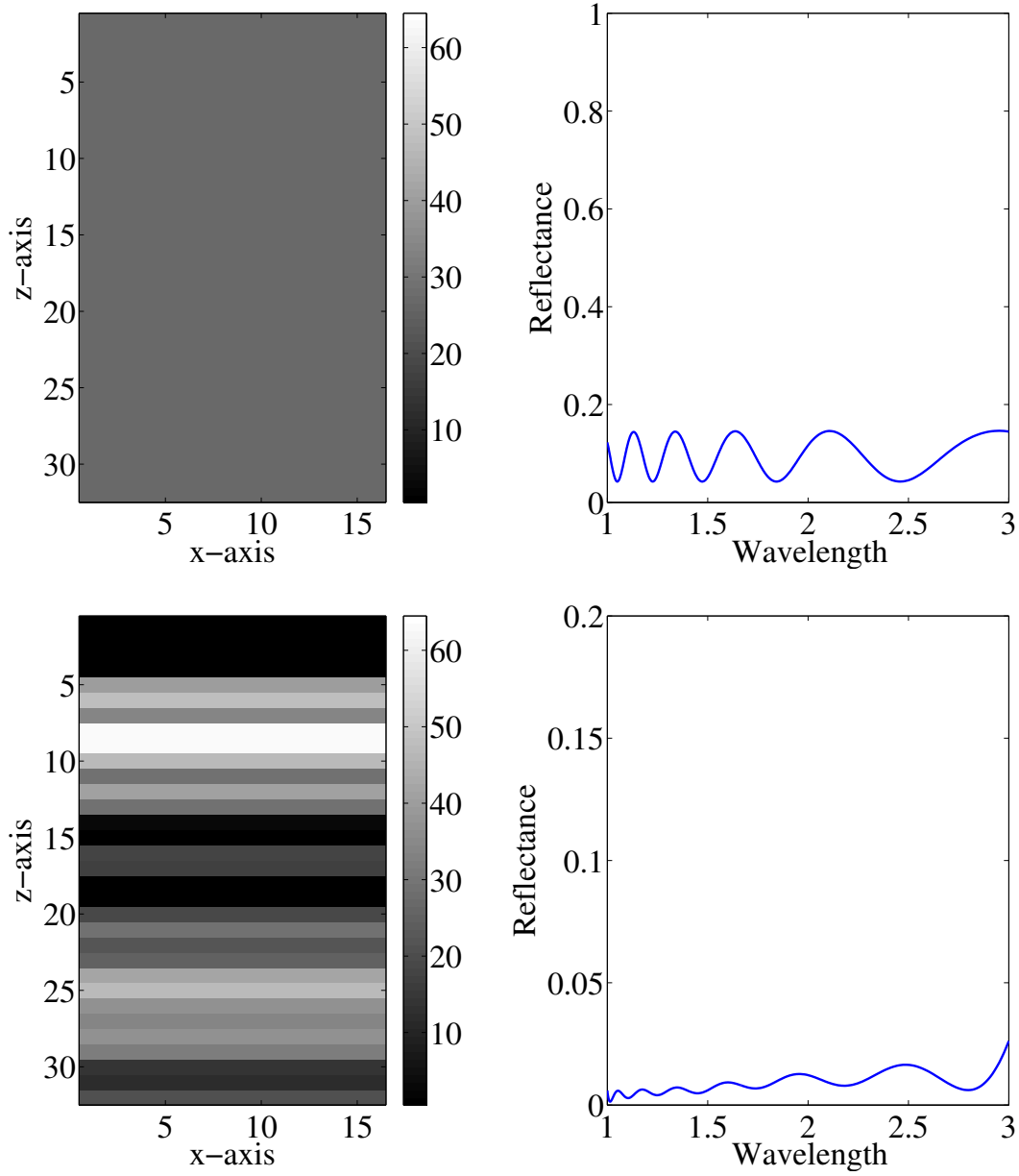
Figure 6.2: Refractive-index profiles and reflectance curves for a broadband antireflection coating with the homogeneous profile as the initial guess. Top: initial guess; Bottom: optimized.

z-axis. This is expected and proofs the validity of our computation of the gradient and the algorithm. The initial guess is a layered structure, therefore the gradient of R_0 should be the same as if we are solving a layered problem. So the gradient will be zero along the x-axis and the next iteration will stay as a layered structure. This implies we can never achieve better performance if the initial guess is a multilayer structure. Indeed, the reflectance curve in Figure 6.2 is similar to and no better than those obtained from the optimization of a pure multilayer coating with similar physical parameters.

Therefore to obtain a solution that is not a multilayer, we need select the initial guess to be non-multilayer. In the next example, we choose the initial guess to be have a rectangular profile, i.e.

$$\varepsilon(x, z) = \begin{cases} \varepsilon_L, & x \in (0, \Lambda/2), \\ \varepsilon_H, & x \in (\Lambda/2, \Lambda). \end{cases}$$

The refractive-index profiles and reflectance curves for the initial guess and optimized solution are shown in Figure 6.3. First of all, notice the distinct feature of the reflectance curve for the initial guess, i.e. the sharp peaks. The existence of these peaks is due to the resonance effect of diffraction gratings. The interested reader is referred to Bao and Ramdani [18], Bao and Huang [16, 17] and the references cited therein for the theoretical justification and applications of this effect. The references just mentioned also considered the optimal design of the resonance effect, i.e. find a grating profile so that the peaks appear at desired locations and whose width are as small as possible.

Notice the peaks are not present in the reflectance curves when the profile is homogeneous. This is because a diffraction grating with a homogeneous profile is indeed not a periodic but layered structure, so the resonance effect will not occur.
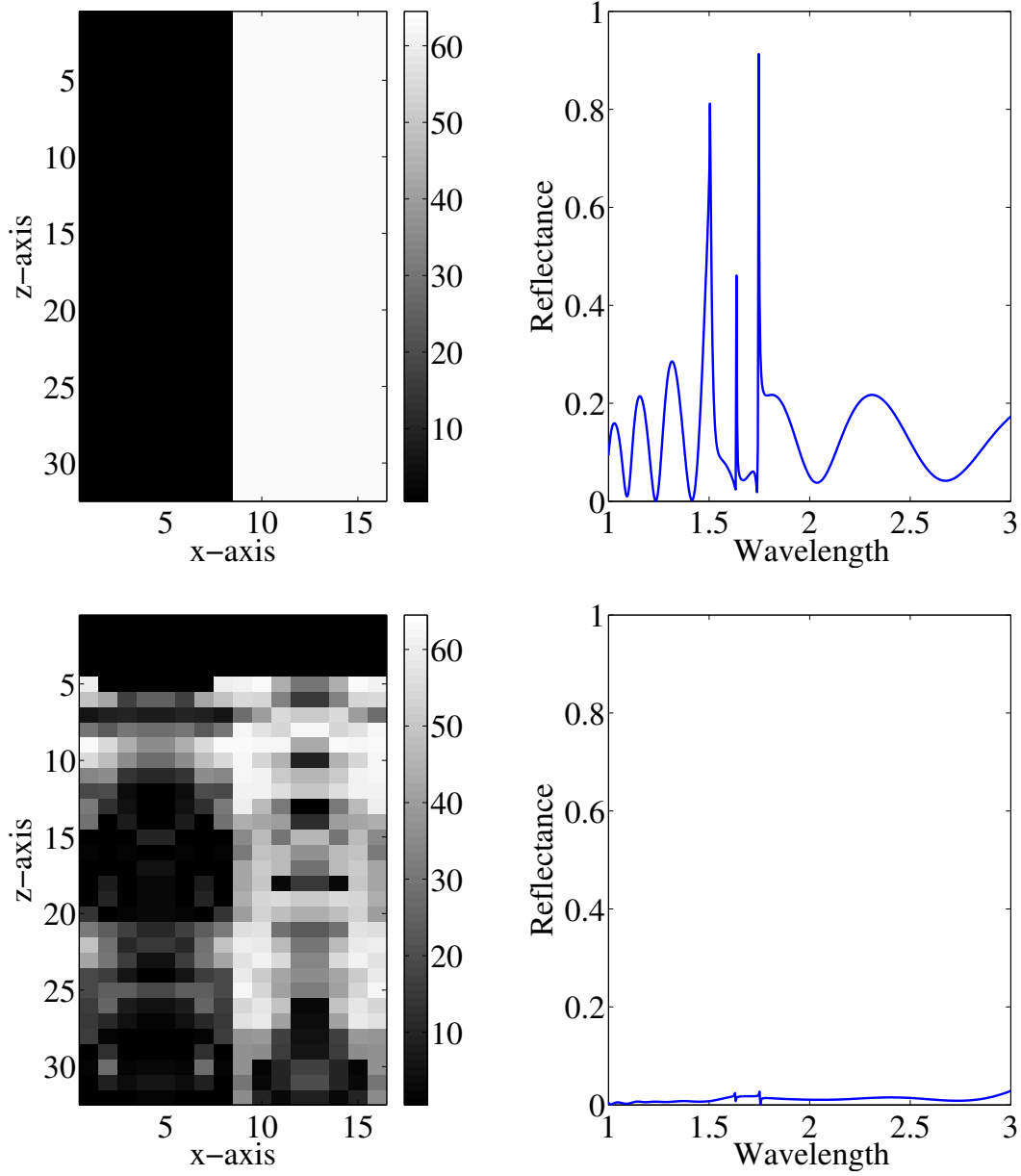
Figure 6.3: Refractive-index profiles and reflectance curves for a broadband antireflection coating with the rectangular profile as the initial guess. Top: initial guess; Bottom: optimized.

For the purpose of antireflection coatings, the peaks should be suppressed as much as possible. This is indeed the case in the for the optimized profile in Figure 6.3, where not only the peaks are suppressed but also the average reflectance is reduced significantly. In fact, the reflectance curve is pretty much on the same level as that obtained with a homogeneous initial guess. On the other hand, the refractive-index profile is not a multilayer and very different from that obtained with a homogeneous initial guess.

Next we choose the initial guess to be a triangular profile, i.e.

$$\varepsilon(x, z) = \begin{cases} \varepsilon_L, & z > \dfrac{4b}{\Lambda}\left(x - \dfrac{\Lambda}{4}\right) \text{ or } z > -\dfrac{4b}{\Lambda}\left(x - \dfrac{3\Lambda}{4}\right), \\ \varepsilon_H, & \text{else}. \end{cases}$$

Figure 6.4 shows the refractive-index profiles and reflectance curves for the initial guess and optimized solution. Like the case when the initial guess is rectangular, the reflectance curve in this case also possesses sharp peaks. They are suppressed in the optimized solution, but not as well as in the previous experiment. The average reflectance, however, is pretty much the same as other examples.
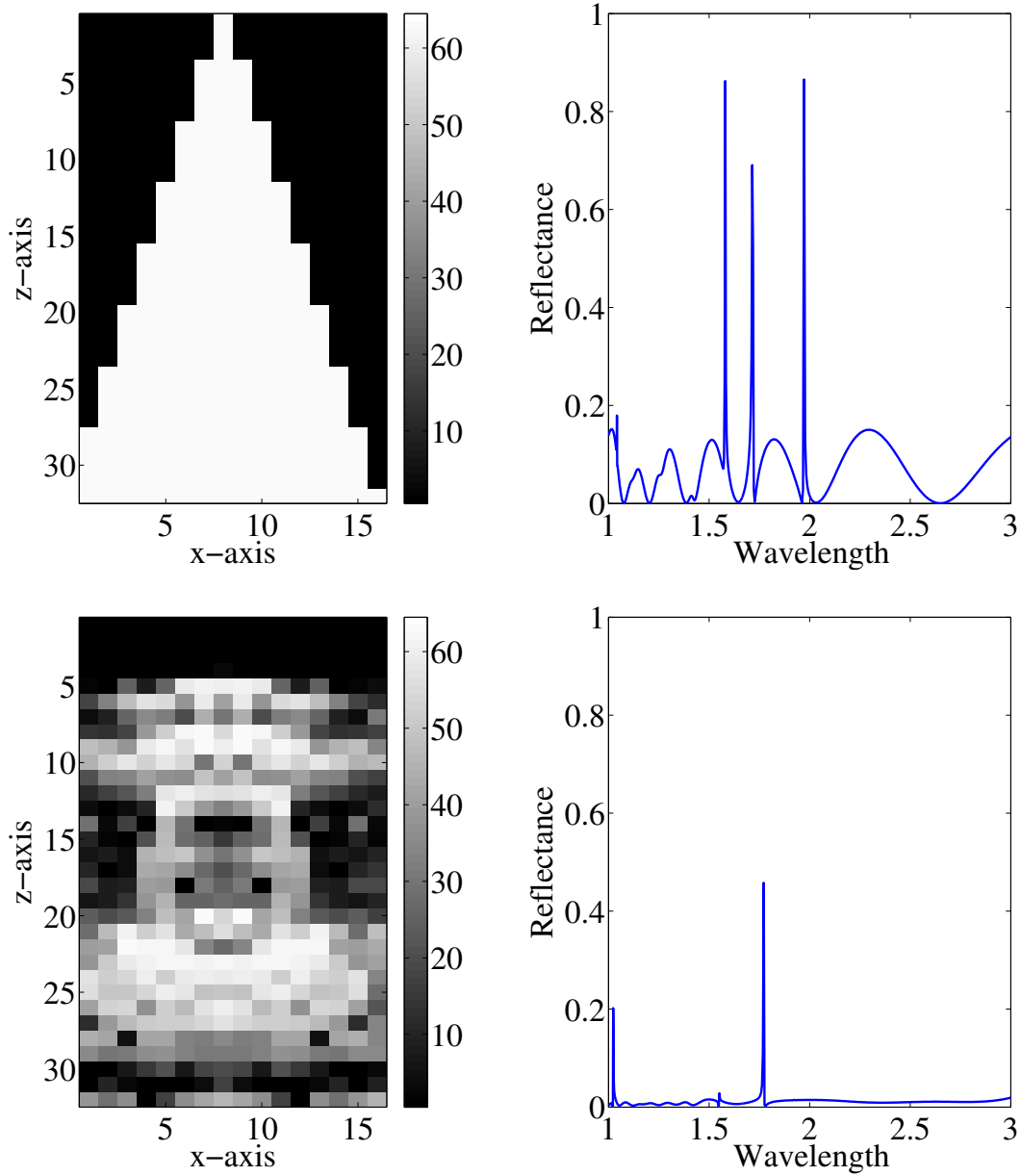
Figure 6.4: Refractive-index profiles and reflectance curves for a broadband antireflection coating with the triangular profile as the initial guess. Top: initial guess; Bottom: optimized.

Chapter 7

Future Work

Much of the work in this dissertation is not completely finished and there are quite a few open problems and new directions that I would like to consider in the future. The topics include but are not limited to the following

- Theoretical justification of the observations made on the effect of the objective functions. We shall investigate in depth the properties of the objective functions in the context of optical coatings. We hope the investigations not only help us understand the effect but also provide guidelines and even new algorithms for numerical computations.

- Extend the study on the effect of objective functions to other types of coatings such as mirrors, bandpass filters and edge filters. We believe similar effects will be observed.

- Use of different metrics in different parts of the spectral or angular region of interest. In the experiments with broadband AR coatings, for example, the reflectance is usually larger towards the longer wavelength region if p is small. By using larger value for p, the reflectance is more evenly spread out, at the cost of higher reflectance in the shorter wavelength region and a higher average value. We propose using smaller values for p in the shorter wavelength region and larger values in the longer wavelength region. We hope this will suppress the heightening and keep the average low at the same time.

- In the design of rugate coatings by penalty terms, I would like to derive theoretical

or empirical expressions relating the performance to the parameters, especially the weight factor α. Such expressions enable users to determine the best value of α for their practical needs.

- In the design of rugate coatings by penalty terms, we found the optimization algorithm converges faster as the weight factor α increases. Since the convergence is faster for larger α, I also plan to devise algorithms in which α is gradually decreased during the optimization in order to increase the speed of convergence for small α or find better solutions.

- We have already seen that good rugate coatings can be obtained by stopping the iteration prematurely when we use global basis functions to discretize the refractive-index profile. We shall consider adding a penalty term to see what solutions we can obtain as in the case where the profile is discretized by local basis functions.

- The diffraction gratings considered in this dissertation have the most general profile, i.e a 2D function. This poses difficulties in terms of both feasibility and numerical computations. It seems more practical to consider diffraction gratings defined by interface, i.e. a 1D function. The optimal design of such type of gratings have been considered in [15, 8, 14, 13] but only at a single frequency. We shall consider the broadband, omnidirectional and other more complicated situations.

- Optimal design problems are closely related to inverse problems. Recently a study [36] showed the methods for inverse problems can be successfully applied for the optimal design of layered structures. I will consider extending them to the optimal design of diffraction gratings.

- Recently it has been shown the methods of recursive linearization are very effective for inverse problems in diffractive optics [39, 40]. The problems considered there use input data at multiple frequencies, thus it is similar to the optimal design of broadband coatings. I plan to adopt this idea to the optimal design of not only diffraction gratings but also layered structures.

- Optimal design of 3D diffraction gratings. The computational cost will increase dramatically and we shall investigate numerical tricks such as increasing the discretization level and convergence tolerance progressively.

BIBLIOGRAPHY

BIBLIOGRAPHY

[1] Sh. A. Furman and A. V. Tikhonravov. *Basics of Optics of Multilayer Systems.* Gif-Sur-Yvette, Edition Frontieres, 1992.

[2] H. A. Macleod. *Thin-Film Optical Filters, Third Edition.* Taylor & Francis, 2001.

[3] P. Baumeister. Design of multilayer filters by successive approximations. *J. Opt. Soc. Am.*, 48(12):955–957, Dec 1958.

[4] J. A. Dobrowolski and R. A. Kemp. Refinement of optical multilayer systems with different optimization procedures. *Appl. Opt.*, 29(19):2876–2893, Jul 1990.

[5] A. V. Tikhonravov. On the synthesis of optical thin films using optimality conditions. *Vestn. Mosk. Univ. Fiz. Astronomiya*, 23:91–93, 1982.

[6] A. V. Tikhonravov. Some theoretical aspects of thin-film optics and their applications. *Appl. Opt.*, 32(28):5417–5426, Oct 1993.

[7] D. C. Dobson. Optimal design of periodic antireflective structures for the helmholtz equation. *European Journal of Applied Mathematics*, 4:321–339, 1993.

[8] D. C. Dobson. Optimal shape design of blazed diffraction gratings. *Appl. Math. Optim.*, 40:61–78, 1999.

[9] G. Bao, D. C. Dobson, and J. A. Cox. Mathematical studies in rigorous grating theory. *J. Opt. Soc. Am. A*, 12(5):1029–1042, May 1995.

[10] M. Born and E. Wolf. *Principles of Optics: Electromagnetic Theory of Propagation, Interference and Diffraction of Light (7th Edition).* Cambridge University Press, 7th edition, 1999.

[11] P. G. Verly. Modified needle method with simultaneous thickness and refractive-index refinement for the synthesis of inhomogeneous and multilayer optical thin films. *Appl. Opt.*, 40(31):5718–5725, Nov 2001.

[12] C. Sanderson. Armadillo: C++ linear algebra library. `http://arma.sourceforge.net`.

[13] G. Bao. Inverse and optimal design problems in diffractive optics. In Y. Hon, M. Ya-mamoto, J. Cheng, and J. Lee, editors, *Recent Developments in Theories & Numerics, Proceedings of the International Conf. on Inverse Problems*, pages 7–46. World Sci., Hong Kong, 2003.

[14] G. Bao and E. Boneetier. Optimal design of periodic diffractive structures. *Appl. Math. Optim.*, 43:103–116, 2001.

[15] G. Bao and D. C. Dobson. Modeling and optimal design of diffractive optical structures. *Survey on Industrial Math*, 8:37–62, 1998.

[16] G. Bao and K. Huang. Optimal design of guided mode grating resonance filters. *IEEE Photonic Tech. Lett.*, 16(1):141–143, 2004.

[17] G. Bao and K. Huang. Computational design for guided-mode grating resonances. *J. Opt. Soc. Am. A*, 22(7):1408–1413, Jul 2005.

[18] G. Bao and K. Ramdani. Resonant frequencies for diffraction gratings. *Applied Mathematics Letters*, 15:755–760, 2002.

[19] G. Bao, K. Huang, and G. Schmidt. Optimal design of nonlinear diffraction gratings. *J. Comput. Phys.*, 184:106–121, 2003.

[20] J. A. Dobrowolski. Completely automatic synthesis of optical thin film systems. *Appl. Opt.*, 4(8):937–946, Aug 1965.

[21] A. V. Tikhonravov, M. K. Trubetskov, T. V. Amotchkina, M. A. Kokarev, N. Kaiser, O. Stenzel, S. Wilbrandt, and D. Gäbler. New optimization algorithm for the synthesis of rugate optical coatings. *Appl. Opt.*, 45(7):1515–1524, March 2006.

[22] R. Fletcher. *Practical methods of optimization*. Wiley, New York, 2nd edition, 1987.

[23] G. Erdmann and F. Santosa. Minimax design of optically transparent and reflective coatings. *J. Opt. Soc. Am. A*, 21(9):1730–1739, Sep 2004.

[24] A. Premoli and M. L. Rastello. Minimax refining of optical multilayer systems. *Appl. Opt.*, 31(10):1597–1605, Apr 1992.

[25] A. Premoli and M. L. Rastello. Minimax refining of wideband antireflection coatings for wide angular incidence. *Appl. Opt.*, 33(10):2018–2024, Apr 1994.

[26] S. G. Johnson. The nlopt nonlinear-optimization package. `http://ab-initio.mit.edu/nlopt`.

[27] D. C. Liu and J. Nocedal. On the limited memory bfgs method for large scale optimization. *Mathematical Programming*, 45:503–528, 1989. 10.1007/BF01589116.

[28] D. Kraft. Algorithm 733: Tompfortran modules for optimal control calculations. *ACM Transactions on Mathematical Software*, 20(3):262–281, 1994.

[29] P. G. Verly. Optical coating synthesis by simultaneous refractive-index and thickness refinement of inhomogeneous films. *Appl. Opt.*, 37(31):7327–7333, Nov 1998.

[30] T. V. Amotchkina. Empirical expression for the minimum residual reflectance of normal- and oblique-incidence antireflection coatings. *Appl. Opt.*, 47(17):3109–3113, 2008.

[31] A. V. Tikhonravov, M. K. Trubetskov, T. V. Amotchkina, and J. A. Dobrowolski. Estimation of the average residual reflectance of broadband antireflection coatings. *Appl. Opt.*, 47(13):C124–C130, 2008.

[32] R. Willey. Predicting achievable design performance of broad-band antireflection coatings. *Appl. Opt.*, 32:5447–5451, 1993.

[33] R. Willey. Refined criteria for estimating limits of broad-band ar coatings. *Proc. SPIE*, 5250:393–399, 2004.

[34] J. A. Dobrowolski, A. V. Tikhonravov, M. K. Trubetskov, B. T. Sullivan, and P. G. Verly. Optimal single-band normal-incidence antireflection coatings. *Appl. Opt.*, 35(4):644–658, Feb 1996.

[35] A. V. Tikhonravov and M. K. Trubetskov. Modern design tools and a new paradigm in optical coating design. *Appl. Opt.*, 51(30):7319–7332, Oct 2012.

[36] S. W. Anzengruber, E. Klann, R. Ramlau, and D. Tonova. Numerical methods for the design of gradient-index optical coatings. *Appl. Opt.*, 51(34):8277–8295, Dec 2012.

[37] B. G. Bovard. Rugate filter theory: an overview. *Appl. Opt.*, 32(28):5427–5442, October 1993.

[38] A. V. Tikhonravov, M. K. Trubetskov, and G. W. DeBell. Application of the needle optimization technique to the design of optical coatings. *Appl. Opt.*, 35(28):5493–5508, Oct 1996.

[39] G. Bao, P. Li, and J. Lv. Numerical solution of an inverse diffraction grating problem from phaseless data. *J. Opt. Soc. Am. A*, 30(3):293–299, March 2013.

[40] G. Bao, P. Li, and H. Wu. A computational inverse diffraction grating problem. *J. Opt. Soc. Am. A*, 29(4):394–399, April 2012.